POLITECNICO
MILANO 1863

SCUOLA DI INGEGNERIA INDUSTRIALE
E DELL'INFORMAZIONE

Study of Reverse Water Gas Shift (RWGS) reaction over Cu-Fe/CeO_2 catalysts

Tesi di Laurea Magistrale in
Chemical Engineering

Author: **Carlo Sala**

Student ID: 970142
Advisor: Prof. Luca Lietti
Co-advisors: Prof. Efthymios Katarelis (KTH), Prof. Lars Petterson (KTH)
Academic Year: 2021-22

Abstract

Reverse Water Gas Shift Reaction (RWGS) is an attractive solution for CO2 utilization and consecutive reduction of emissions into the atmosphere. This reaction is limited by thermodynamics while there are problems with its implementation at large scale. In order to improve the process feasibility it is necessary to develop an efficient and effective catalyst. Contrary to typical studies where catalytically active metals are deposited on inert supports, in this work the investigation of a bimetallic (Fe-Cu) catalyst on active support was carried out. In particular, the RWGS reaction was studied over Cu-Fe/CeO2 catalyst with and without potassium promotion by means of catalytic activity tests in a fixed bed reactor. The catalysts were synthesized by hydrothermal method and successive impregnation of active metals. All the materials were characterized through BET analysis, H2 temperature programmed reduction, X-ray diffraction and ICP-MS elemental analysis. The effect of temperature and H2/CO2 inlet molar ratio was assessed. Experimental results showed that Cu-Fe combination exhibits considerable catalytic activity at temperatures greater than 500°C. CO2 conversions from 24% to 100% of the equilibrium conversion were achieved at gas hourly space velocities of 360 000 h^{-1}. Selectivity to CO varied between 70-90%. Potassium promotion plausibly results into a partial coverage of active sites, thus leading to lower conversion (10%- 50% of the equilibrium value). Long term runs (69-100h) did not show any sign of deactivation nor selectivity loss for the unpromoted catalysts, while the K-promoted catalyst exhibited a slow activity decay probably due to sintering.

Keywords: CO_2 utilization, RWGS, Catalyst, Characterization, Synthesis, Bimetallic catalyst, Active catalytic support.

Abstract in lingua italiana

La reazione di Reverse Water Gas Shift (RWGS) costituisce una possibile soluzione per l'utilizzo di CO2 e per la riduzione di emissioni di gas serra in atmosfera. Tale reazione è limitata termodinamicamente e l'applicazione su grande scala presenta diversi ostacoli. Per migliorarne l'applicabilità su scala industriale, è necessario disporre di un catalizzatore attivo e selettivo. Contrariamente alle tecnologie solitamente impiegate, in cui metalli attivi sono depositati su supporti inerti, in questo studio è stato investigato un catalizzatore bimetallico (Fe-Cu) con supporto attivo. In particolare, la RWGS è stata studiata su un catalizzatore Cu-Fe/CeO2, inoltre è stato analizzato l'effetto del potassio come promotore. L'attività catalitica dei campioni è stata testata in un reattore a letto fisso. I catalizzatori sono stati sintetizzati tramite "hydrothermal method" e successivo deposito dei metalli attivi. I materiali così ottenuti sono stati caratterizzati tramite analisi BET, riduzione programmata con H2, diffrazione ai raggi X e analisi elementare ICP-MS. Inoltre, è stata analizzata l'influenza del rapporto molare H2/CO2 in alimentazione. I risultati sperimentali hanno riportato un'elevata attività della coppia Cu-Fe a temperature superiori a 500°C. Con una velocità spaziale di 360 000 h^{-1}, sono state raggiunte conversioni tra il 24% e il 100% del valore di equilibrio e selettività verso CO comprese tra 70% e 90%. L'aggiunta di potassio ha prodotto una minore conversione (10%-50% del valore di equilibrio), probabilmente a causa dell'ostruzione dei siti attivi. Alcune prove catalitiche a lunga durata (69-100h) non hanno riportato disattivazione o perdita di selettività per i campioni senza potassio, mentre l'aggiunta del promotore è risultata in una lenta perdita di attività, probabilmente a dovuta al fenomeno di "sintering".

Parole chiave: Utilizzo di CO_2, RWGS, Catalizzatore, Caratterizzazione, Sintesi, Catalizzatore bimetallico, Supporto catalitico attivo.

Contents

1 | Introduction

1.1. Background

It has been extensively reported that the anthropogenic activity during the last century has lead to a dramatic increase of the carbon dioxide (CO_2) content into the atmosphere altering the natural carbon cycle equilibrium [1]. The consequences of this rapid change are negative under both the economical and environmental point of view. This is displayed clearly by the average temperature increase and the acidification of the oceans, together with the more frequent extreme weather events and the rapidly increasing ice melting [2]. In order to face this problem, the reduction of the emissions of carbon dioxide into the atmosphere is the first action that must be undertaken. For this purpose, research is studying alternative paths for chemical synthesis and energy production solutions with reduced carbon footprint in order to avoid the formation of CO_2 in the first place. However some emissions of carbon dioxide cannot be prevented, at least in the short term, since they mainly derive from the exploitation of the fossil fuels as main source of energy and as fundamental source of raw materials for the chemical industry, and as of now, the shift towards alternative sources is too slow to be considered as a ready solution to the environmental issue. Hence, in this context, capturing the carbon dioxide becomes a good opportunity to avoid its release into the atmosphere.
The captured CO_2 can undergo storage or utilization. From one side the sequestration places risks of leaks and its consequences on the environment are not easy to evaluate [3]. On the other hand, the utilization of the captured carbon dioxide appears more interesting, because it takes advantage of CO_2 as a carbon resource instead of considering it as a waste [4], moreover it is strongly more appealing for reducing the net amount of CO2 emissions compared to sequestration [5, 6]. This solution, indeed, introduces the possibility to switch from a linear carbon economy to a circular one [7] helping to re-establish the natural carbon cycle conditions with the possibility of obtaining a positive cash flow from the production of useful products starting from CO_2 as raw material. CO_2 is one of the most abundant and cheap sources of carbon in nature and it is already employed in some processes such as urea production, where it is one of the main reactant,

and methanol synthesis, where it is added to the main reactants. Anyway the overall CO_2 consumption by chemical industry balances just a small amount of the emissions and an attractive solution for carbon dioxide utilization is to use it as feedstock for fuel and chemical synthesis. In particular this process includes the reduction of carbon dioxide via direct or indirect methods, where the most feasible solution comparing the technical challenges is the indirect thermochemical reduction of carbon dioxide [6]. Indeed there is already a wide know-how on this process thanks to many research works on the conversion of CO_2 over heterogeneous catalysts. Among the possible reactions, the main products that can be obtained are CO via RWGS (Reverse Water Gas Shift) reaction, Methanol and hydrocarbons. The first process, produces carbon monoxide, which is a very reactive $C1$ compound widely adopted in the chemical industry. For example it can be used as feedstock in the production of $MeOH$ through the typical catalytic process on $Cu/ZnO/Al_2O_3$ catalysts, it can be adopted for the production of synthetic hydrocarbons of various length through the Fischer-Tropsch (FT) synthesis [8], or it is a reactant for the acetic acid production via Monsanto or Cativa processes. The direct conversion of CO_2 via FT or methanol synthesis could be considered a better way to obtain straight away the desired product instead of having an intermediate stage, hence improving the efficiency of the overall process. The direct production of $MeOH$ allows to obtain a valuable product with multiple uses such as fuel additive and feedstock for the production of many chemicals, but in order to develop an efficient process starting from CO_2, the yield and selectivity of this reaction should be improved significantly, while keeping reasonable the overall cost for the process. The synthesis of alkanes and olefins directly from CO_2 via FT reaction is very attractive because it is not as limited as the RWGS from a thermodynamic point of view and because it is an exothermic reaction (as well as the methanol production). The main technical challenge to be overcome for the feasibility of this process is the synthesis of active water resistant catalysts (since water is the main byproduct of the reaction). But the studies in this field are still at a preliminary level and CO_2-based Fischer-Tropsch is the least studied process between the ones mentioned above [9]. After these considerations, we can state that among the reported alternatives the production of CO via RWGS is a flexible choice because it allows for the production of a fundamental feedstock for the further synthesis of different valuable chemicals exploiting the already existing industrial infrastructure. Moreover, the employment of CO can be adapted depending on the market request. RWGS reaction has received a lot of attention during the last years because it appears as a key stage in the conversion of CO_2 to more reduced products , as a matter of facts, it seems to be the first step for further transformations such as to methanol or hydrocarbons. Hence the study and understanding of this specific reaction is crucial for the development of future

efficient processes which directly convert CO_2 into final products.

1.2. The Reverse Water Gas Shift reaction

The RWGS reaction consists of the hydrogenation of CO_2 to CO, producing water as a byproduct (eq.1.1).

$$CO_2 + H_2 \leftrightarrow CO + H_2O \qquad \Delta H = 41.3 kJ/mol \tag{1.1}$$

In a reacting system containing the chemical species reported above, a second reaction can take place: the Sabatier reaction, also known as methanation of CO_2 (eq.1.2).

$$CO_2 + 4H_2 \leftrightarrow CH_4 + 2H_2O \qquad \Delta H = -164.7 kJ/mol \tag{1.2}$$

These two reactions compete for the consumption of carbon dioxide. An other possible product is methanol, but its production is strictly related to the pressure of the reacting system, as a matter of fact, the conversion of CO_2 into methanol requires high pressures [10]. The RWGS reaction does not show any change in the total number of moles, while the Sabatier reaction takes place with a reduction in the number of moles. Which means, that from a thermodynamic viewpoint, RWGS is not affected by pressure, while Sabatier reaction is favored at high pressures. Thus, working at low pressures, for example close to atmospheric value, is a good strategy to favor the selective conversion of carbon dioxide to CO instead of CH_4. Regarding methanol, its formation at atmospheric pressure is not observed [10]. Concerning the temperature effect on the thermodynamic equilibrium of the system, the RWGS reaction is favored at high temperatures, while the methanation is favored at low temperatures. Hence we expect that a reacting environment at high temperature will be more selective towards CO. The conversion of CO_2 and selectivity towards CO at equilibrium conditions are reported in Figure 1.1 (A,B). These thermodynamic results were taken from literature. Different ratios of hydrogen and carbon dioxide in the feed have been considered, in particular H_2/CO_2=1, 2, 4, 6, 8 (molar ratio). From a thermodynamic point of view, considering the stoichiometric coefficients of the two involved reactions, a higher conversion of CO_2 is expected increasing the amount of hydrogen while at the same time favoring the production of CH_4.

Observing Figure 1.1 (A,B) it is possible to identify a general behaviour among the different ratios. Conversion decreases while increasing temperature in the low range, then increases facing higher temperatures. While at the same time selectivity towards CO increases with temperature (Figure 1.1 (D)). This aspect can be explained by considering

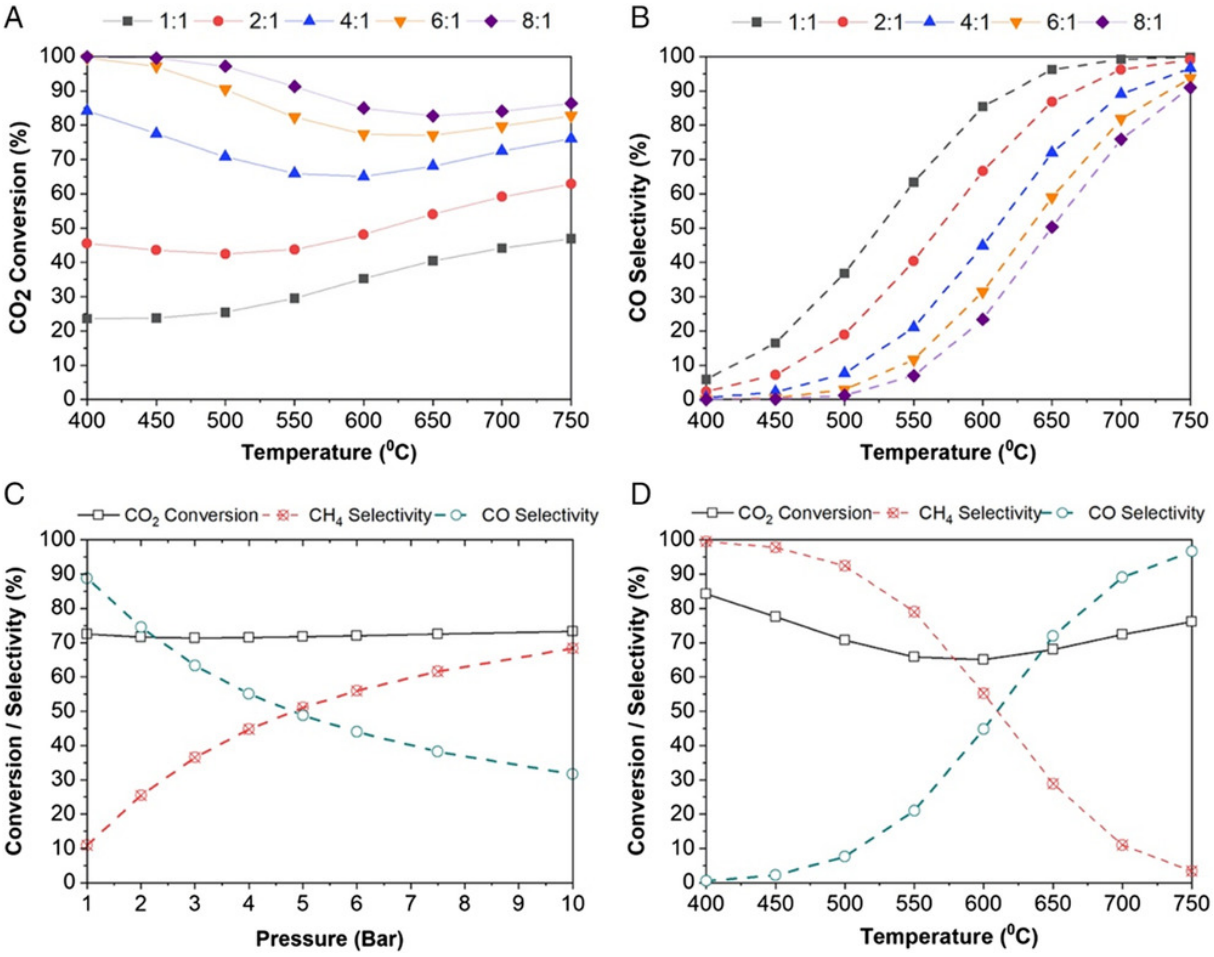

Figure 1.1: Equilibrium conversion of CO_2 and selectivity towards CO at different H_2/CO_2 ratios as a function of temperature. Image taken from [2].

the exothermicity of Sabatier reaction, compared to the endothermicity of RWGS. Further analysis of the thermodynamic equilibrium conditions will be performed in Section 3.1. Regarding the pressure effect on the reacting system, no relevant change in equilibrium conversion is observed within a pressure range from 1 to 10 bar (Figure 1.1 (C)). On the other hand, selectivity is strongly affected by pressure. Given of the change in number of moles of methanation reaction we expect an increase in CH_4 selectivity as pressure increases. This can be clearly observed, where the selectivity towards CO drops as pressure increases. These analyses of pressure variation were obtained considering a H_2/CO_2 inlet ratio of 4 as it is reported to give a syngas with a suitable composition to feed a methanol synthesis reactor (after the removal of water).
It is clear that the main intrinsic limitations of the RWGS reaction are the equilibrium conversion, which is hindered by thermodynamics, and the selectivity to CO, which is in competition with the production of methane. The conversion at equilibrium condition of the system can be improved by working at high temperatures, and increasing the amount of hydrogen in the feed. This solution provides an additional advantage because some of the unreacted hydrogen could be found in the outlet of the reactor, thus giving already a syngas with a determined composition. The drawback is that hydrogen comes with a cost, which actually represents the main factor to the economical feasibility of this reaction as it will be explained in Section 1.5. Hence the benefits coming by adopting a larger hydrogen amount should be balanced with the additional expenses that it implies. An other option could be subtracting one of the reactants from the reacting environment in order to push the equilibrium conversion. For example water can be removed by means of a selective membrane reactor, but this kind of solutions are still under development [11]. Alternatively, performing two reactions in series in the same reactor seems a promising strategy to achieve greater efficiencies. Indeed, tandem catalytic schemes would allow to consume directly the produced CO pushing the RWGS equilibrium towards the products, while producing the desired chemical species with no need for an intermediate step. The most suitable applications are the coupling of Fischer-Tropsch reaction or Methanol synthesis to RWGS. These combinations would also bring a beneficial effect from the thermal point of view, since the first endothermic reaction would be coupled with exothermic reactions (FT or MeOH synthesis), eliminating or reducing the need for an external heat supply [2]. Even though these tandem catalytic configurations seem the most promising technologies for the hydrogenation of CO_2, their development has to overcome the technological obstacle of synthesizing a catalyst suitable for both the involved reactions. Which means guaranteeing good performances at operating conditions that are not ideal, since a trade-off between the optimal values of temperature and pressure for the two reactions must be selected. At the same time improvements must be done in order to be

able to manage these complex processes. An additional way to improve the equilibrium conversion of the RWGS reaction consists of introducing a recycle after the reactor which brings back to the inlet part of the unreacted reagents by previous condensation of water. This allows for a higher overall conversion, but of course the process configuration is more complicated. Hence, once again, the benefits should be balanced with the additional costs that they involve [7]. In literature an optimized implementation of a subsequent RWGS and methanol synthesis is available and well studied. It is the CAMERE process (carbon dioxide hydrogenation to form methanol via reverse-water-gas-shift reaction). It consists of a reverse water gas shift reactor followed by a methanol synthesis reactor with an intermediate water condensation system. The selectivity to CO of the first reaction is fundamental in order to achieve a sufficient production of methanol [12]. Notably, under some specific reacting conditions this process configuration is reported to have a methanol yield 20% higher with respect to the direct conversion of CO_2 to methanol [8].
In light of the general considerations reported about RWGS reaction, it results that there is a wide range of possibilities to develop this process in order to make it an efficient and effective way to achieve a net reduction of CO_2 emissions by producing valuable chemicals, although a deeper study of the reaction mechanism and the synthesis of more efficient and selective catalysts are fundamental in order to transfer this solution to large scale applications.

1.3. Types of catalysts for RWGS

In order to enhance the reaction rate of RWGS reaction by promoting a lower activation energy reaction path, a catalyst should present two different functionalities. It must be able to adsorb CO_2 allowing for the cleavage of one of the two $C = O$ bonds, and it should also have some available sites for the dissociative adsorption of H_2. Moreover these two functionalities should be correctly balanced in order to favor CO as the main final product. For example, an excessive hydrogenating activity might lead to more hydrogenated products with respect to CO, such as methane. Hence the different catalytic activities must be tuned properly [6].
In order to fulfill these characteristics, research identified oxide catalysts as suitable candidates because they presented both these functionalities, in particular thanks to their abundant oxygen vacancies, for example ZnO, CeO_2 and Al_2O_3 have been studied [1]. These type of catalysts demonstrated good selectivity towards CO but at the same time their ability in activating CO_2 was limited, moreover they suffered from sintering at high temperatures (which might be adopted as operating condition when high conversions are needed). Subsequently, more advanced types of oxides were investigated, such as spinel

and perovskites type oxides [1]. They guaranteed a good reversible oxygen storage capacity, which is the main parameter that affects the activity towards CO_2 adsorption and breakage, because the oxygen vacancies are able to host an oxygen atom of the CO_2 molecule. Together with this feature, the complex oxides presented good structural stability at high temperatures. More recently research has moved towards the application of metallic catalysts deposited on supported metal oxides, in fact they are relatively easy to synthesize and they present promising activity thanks to the metal-support interfaces, which proved to be a suitable site for the activation of CO_2. The drawback for these type of catalysts is tuning their different activities, indeed the metal site should be able to dissociate hydrogen molecules while at the same time allowing hydrogen atoms to migrate towards the nearby oxygen vacancies where CO_2 has been adsorbed in order to perform the RWGS reaction. On the other hand, the hydrogenating power should be tuned correctly because it would otherwise bring to excessive hydrogenation, whose main product is methane, thus leading to a loss in selectivity [13, 14]. Metal oxides are usually adopted as support for metal based catalysts because of their capability of enhancing the reaction performances while offering a solid support for the active phase. There are two main types of metal oxides supports: reducible (CeO_2, TiO_2) and irreducible (SiO_2, Al_2O_3) supports. Irreducible supports participate indirectly to the reaction by guaranteeing a good CO_2 adsorption capability but they do not have significant activity on their own [4]. On the other hand, reducible supports are able to create oxygen vacancies which are suitable for CO_2 strong adsorption and activation. These vacancies are likely to be additional active sites for the RWGS reaction, hence the turnover frequency (TOF) on reducible supports is strongly enhanced. For example Pt/TiO_2 has eight times the TOF of Pt/Al_2O_3 and Cu/CeO_2 is four times more active than Cu/SiO_2 [4]. Thus reducible oxides are more suitable for RWGS application, but their features should be tuned carefully because they are more likely to loose selectivity to CO in favor of CH_4. This tendency is strongly affected by the type of active metal.

Concerning the metal which establishes the actual active phase of the supported catalysts, in the first place precious metals where considered as suitable candidates. In particular Pt, Au, Pd and Rh present excellent activity [15].On the other hand the high price of these elements and their tendency to sinter at high temperature limit the feasibility of their employment on industrial scale processes. Nonetheless Pt and Rh have been identified as the most performing precious metals and their properties can be improved by tuning properly the catalytic features. Therefore, given the problems related to precious metals, transition metals have been identified as a possible alternative. In particular Ni has been studied because of its very high activity, but it presents an excessive hydrogenating power, thus leading mainly towards methane selectivity [15, 16]. Copper is an other

interesting active phase able to perform the RWGS reaction. Indeed, copper shows good performances both in terms of conversion and selectivity even at low temperature [17, 18]. The problem with this metal is that it easily sinters at high temperature, hence the main challenge to synthesize an efficient Cu-based catalyst is to enhance its thermal stability without losing he catalytic performances [15]. After having acknowledged that many different solutions are available to perform the RWGS reaction, it is clear that there is not a unique substantially best solution. Hence some attempts have been made in order to obtain better performing catalysts overcoming the existing problems. The most common modifications are reported below [4].

- Tuning metal-support interactions: the RWGS reaction takes place at the interface between metal and support, tuning their activity can be of great help in increasing the reaction performances. Maximizing the metal-support interface sites can be done by reducing metal particle size, which also increases the number of surface sites available for the reaction. In general reducing the metal particle size increases selectivity towards CO.
- Addition of reducible transition metal oxide promoters: adding supporting transition metal oxides gives an interaction with the metal since these oxides can form oxygen vacancies similar to those of the reducible supports that play a role in CO_2 activation.
- Bimetallic alloy: depositing two metals in the form of bimetallic alloy can induce stronger adsorption energy of CO_2.
- Addition of alkali metals: these metals, if added to RWGS catalysts, have proven to increase the activity and also shift the selectivity to CO rather than CH_4. The improvement is due to the enhanced reducibility and surface basicity. In particular the adsorption of the acidic CO_2 is favored by higher basicity.
- Enveloping metal particles: by enveloping the metal with nanoporous materials CO production is higher probably because of the hindered interaction between the active site and CO. The result is an increase both in activity and selectivity.

1.4. Mechanism

There is not a uniform opinion in literature about the mechanism followed by RWGS reaction while moving from reactants to products. Different mechanism are reported but in general two main types are assessed as the possible ones. The first considers the evolution of the catalytic cycle through a redox mechanism, also known as dissociative mechanism.

In particular the catalyst, which starts from its reduced form, is oxidized by CO_2 giving CO, while H_2 closes the cycle reducing back the catalyst to its original state, giving water as byproduct.

$$\begin{aligned} &CO_2(g) + 2* \rightarrow CO* + O* \\ &CO* \rightarrow CO(g) + * \\ &H_2(g) + 2* \rightarrow 2H* \\ &2H* + O* \rightarrow H_2O* + 2* \\ &H_2O* \rightarrow H_2O(g) + * \end{aligned} \tag{1.3}$$

The other possibility is the association mechanism, which considers the adsorption of CO_2 on the catalyst surface under the form of formates ($HCOO*$) or carboxyl species ($COOH*$), and their subsequent decomposition produces CO and water [1].

$$\begin{aligned} &H_2(g) + 2* \rightarrow H* + H* \\ &CO_2(g) + * \rightarrow CO_2* \\ &CO_2* + H* \rightarrow HCOO* + * \\ &HCOO*(COOH*) + * \rightarrow HCO*(COH*) + O* \\ &HCO*(COH*) + * \rightarrow CO* + H* \\ &H* + O* \rightarrow OH* + * \\ &H* + OH* \rightarrow H_2O* + * \\ &H_2O* \rightarrow H_2O(g) + * \\ &CO* \rightarrow CO(g) + * \end{aligned} \tag{1.4}$$

The actual type of mechanism depends on the reaction conditions and the type of catalyst. But in general the $HCOO$-mediate mechanism is unlikely to take place because formates are really stable species and therefore hardly reactive, hence their decomposition to give CO and water is not really favored. On the contrary, the redox and carboxyl-mediate paths have been investigated on different metals and it has been found that the type of mechanism is correlated to the oxygen interaction with the active metal, hence it seems not affected by the support. Metals with low oxygen affinity favor the $COOH$-mediate mechanism while metals with strong oxygen affinity favor the redox mechanism. Thus Pt, Pd, Ag are reported to undergo a carboxyl-mediate mechanism, while Cu, Ni, Rh are more feasible for the dissociative mechanism given their stronger metal-oxygen interaction [19–21].

1.5. Economic and sustainable feasibility

In order to assess objectively the performances of a catalyst, a brief discussion is required about the economic and sustainable feasibility of RWGS reaction. This reaction is reported to be a possible contribution for reducing the net emissions of carbon dioxide in the atmosphere. Indeed it could be implied to turn part of the CO_2 emissions into chemicals, reducing the fossil resources demand as raw materials for the chemical industry, partially closing the carbon cycle. In this context the economic feasibility of the whole process is to be taken under consideration. As a matter of fact, even assuming to have an optimal catalyst, RWGS reaction is limited under a thermodynamic point of view, and in order to enhance the productivity high temperatures and high amount of hydrogen are needed. But these two factors contribute heavily to the energetic requirement of the process, which currently comes with substantial CO_2 emissions. At this point, an evaluation of the net emissions reduction compared to the process cost is required.
Hydrogen can be obtained from different sources: blue hydrogen (from fossil sources with capture of the emitted carbon); green hydrogen (from renewable energies, including biomass gasification); grey hydrogen (from fossil sources without capture of the emitted carbon).
Of course the overall assessment of net carbon dioxide consumption should be done considering the final application, thus if RWGS is meant for producing CO or syngas (CO and H_2 mixture in different amounts depending on the final application), indeed they require different concentration of hydrogen in the feed. The general analysis reports that an effective reduction of carbon emissions is observed only when blue or green hydrogen are adopted [2]. On the other hand also emissions related to the energy requirement of RWGS should be taken into account, considering operating temperature and source of heating. In general they are negligible compared to emissions related to hydrogen production if we consider heating duty derived from renewable sources, but they start to be relevant if the energy source is direct combustion or energy taken from the national grid (for example Europe energy grid) [2].
Regarding the cost of the process, hydrogen production is by far the most relevant cost source [2]. As a matter of fact, the expense for hydrogen production is more relevant than the cost associated to CO_2 capture, which is cheaper if carbon dioxide is captured from point sources rather than directly from the atmosphere [2]. The adoption of green hydrogen is far from being economically feasible, while grey and blue hydrogen could lead to a positive cash flow only under specific conditions, and only for the optimized production of CO but not of syngas [2]. In this case, if the produced CO is meant for a process that requires syngas as feedstock, the addition of hydrogen will be required, adding costs and

emissions to the overall balance. On the other hand the application of RWGS for syngas production results into no profit under any condition [2]. In conclusion, in order to make this process economically feasible while achieving an effective reduction of net CO_2 emissions, it is crucial to reduce the cost of green hydrogen by improving renewable energy technologies in the first place, subsequently an optimized catalyst for this reaction should be identified in order to work close to equilibrium conversion with enhanced selectivity to CO, and, in the end, the improvement of CO_2 capture technologies is necessary in order to reduce the overall cost. About these topics research has been moving really fast during the past few years.

1.6. Goal of the thesis work

As explained in Section 1.3, RWGS is a widely known reaction and it has been tested on many supports, active phases and promoters, but, despite very good results were obtained, there is still possibility of improvement. Moreover, in order to make this process feasible from an economical point of view it is necessary to have the best possible performing catalyst, which maximizes the yield of the desired product, thus it is important to test and assess all the suitable catalytic combinations. After the evaluation of the wide range of process and catalytic solutions available for performing the RWGS reaction, this work tried to select a suitable catalyst that could be able to provide good performances in terms of activity and selectivity, while trying to avoid the typical problems related to catalysts for this reaction, sintering and deactivation among the others. This work has been performed at the Process Technology division of Royal Institute of Technology in Stockholm and it can be summarized as follows.

After a literature review about the topic, the novel combination of Cu and Fe on CeO_2 has been chosen as suitable candidate for RWGS reaction. These two metals have been tested in literature separately on reducible supports or together on non reducible support. Hence, the study of this novel bimetallic catalyst, allows for the evaluation of the advantages of $Cu - Fe$ on a reducible active support such as ceria. The effect of K as a promoter has been evaluated on the mentioned bimetallic catalyst.

Concerning the support, CeO_2 has been selected as a good option, first of all because it is a reducible support [4], thus it participates directly to the reaction. Moreover, this support is reported to have an excellent capability of forming oxygen vacancies, which allow for an effective adsorption and activation of the CO_2 molecule. In particular, CeO_2 structure can be modified in order to maximize this effect [22, 23]. This support also presents an interesting behaviour regarding the interaction with active metal particles, since it is able to form some interface structures, which become available sites for the

RWGS reaction. These interface interactions can be ascribed to a Strong Metal Support Interaction (SMSI) [24], resulting in better catalytic performances.
Cu has been selected as main active phase, because it guarantees good performances both in terms of conversion and selectivity while having an accessible cost compared to precious metals [15–17]. Moreover Cu activity has been assessed many times on CeO_2 support and their interaction is well known for activating efficiently the RWGS reaction [25–27]. Nontheless, the main problem reported by the adoption of a copper-based catalyst, is sintering, which occurs at high temperatures, hence the catalyst deactivation is a main issue. In order to prevent the agglomeration of Cu particles on the catalytic surface, other metals can be adopted as stabilizers. In particular the addition of Fe to the system is beneficial for this purpose. Indeed, when added in correct amount, it stabilizes the copper particles, acting like a matrix that inhibits agglomeration. Together with the addition of Fe comes the coverage of some Cu sites, but this does not affect negatively the catalytic performances, as long as the amount of iron is small compared to the amount of copper. Furthermore Fe has an activity in RWGS catalysis on its own, despite it is significantly lower than Cu. The addition of this promoter does not only prevent the deactivation of the catalyst but also improves the catalytic performances of Cu/CeO_2 thanks to the formation of new sites available for the reaction at the interface Fe-Cu. An other reason for the observed performances improvement is that iron has a greater capability of being oxidized, hence, after copper atoms are oxidized by the reaction with CO_2, they are able to transfer oxygen atoms to the neighbouring iron phase, increasing the rate of reduction of Cu, which otherwise takes place only thanks to gas phase H_2 [28, 29].
Other promoting agents are commonly added to RWGS catalysts, in particular alkali metals proved to be suitable for the enhancement of catalytic performances thanks to their tendency to add basicity to the surface hence improving the capability of adsorbing the acidic CO_2 [30, 31]. Potassium has been identified by literature as a suitable candidate among the alkali metals, because it combines a good enhancement of catalytic efficiency while at the same time leaving the capability of adsorbing H_2 unchanged, hence not changing the selectivity towards methane. Regarding the application of potassium to the selected active phases, it is reported that K addition to Cu and Fe based catalysts has proven to be successful [32–34]. Furthermore, other than sintering, deactivation of RWGS catalyst may occur because of coke formation that may take place on catalyst surface [12]. This brings to coverage of active sites and clogging of pores, with the consequent reduction of surface area available for the reaction. Potassium is reported to have a gasifying activity towards coke, hence, it may prevent the catalyst deactivation process ascribed to this phenomenon [35, 36].
Based upon the considerations reported above, the four species CeO_2, Cu, Fe, K, were

selected, each one with its role, as suitable for the purpose of a RWGS catalyst. These species were combined in different amounts to synthesize three different catalysts. The amount of Cu selected was around 8-10% in order to provide the formation of the active sites from the interaction of Cu with CeO_2, while avoiding an excessive surface coverage which inhibits this effect [15]. Literature reports that the optimal amount of Fe to promote the stabilization of copper is within the range 0.3-0.8%. Towards the upper limit of this interval a better activity is observed, while concentrations close to the lower limit provide better deactivation prevention. Thus an intermediate concentration of 0.6% was chosen, in order to balance these two features [28, 29]. In the end, K is reported to be effective in activity promotion if added in weight percentage included between 0.52% and 1.9%. The higher is the amount, the higher is the activity enhancement, but at the same time the higher is the coverage of the main active phase [32]. In conclusion the nominal compositions of the selected catalysts were:

- $Cu - Fe/CeO_2$ (10-0.6/CeO_2)
- $Cu - Fe - K/CeO_2$ (10-0.6-0.52/CeO_2)
- $Cu - Fe - K/CeO_2$ (10-0.6-1.9/CeO_2) [1]

As already mentioned at he beginning of this Section, no existing study on RWGS catalysts with this elemental combination has been found at the time of this research. In particular the adoption of Cu and Fe simultaneously on reducible support is a novelty.
The support has been firstly synthesized, subsequently the deposition of metallic phases was performed, in the end the promoter was added in two different amounts.
In order to evaluate the performances of the synthesized catalysts an experimental setup has been built on purpose. On such setup it has been possible to run experiments to observe the behaviour of the different catalysts. Furthermore characterization analyses have been performed in order to obtain reliable information about the composition and structure of the obtained catalysts.

[1] All numbers are to be intended in weight percentage

2 | Materials and methods

2.1. Thermodynamic analysis

The thermodynamic analysis of the reacting system at equilibrium has been performed considering a system containing the species H_2, CO_2, CO, CH_4, H_2O. In order to solve the equilibrium condition, the value of activity constant and equilibrium constant were equaled for each one of the two reactions required to characterize completely the chemical system 2.3[1]. Ideal mixes of ideal gases were considered. The considered reactions were the RWGS reaction and the Sabatier reaction. This evaluation was done firstly to confirm what reported by literature, and secondly in order to get a further insight on the reaction. In this way a deeper evaluation of the effect of different variables on the system allowed to select suitable operating conditions for the experimental campaign. These aspect will be further discussed in Section 2.5.

$$K_{eq,j} = exp\left(\frac{-\Delta G^0_{R,j}(T,P^0)}{RT}\right)$$
$$where \qquad \Delta G^0_R(T,P^0) = \sum_{i=1}^{NS} \nu_{i,j} \Delta G^0_{f,i}(T,P^0) \tag{2.1}$$

$$K_{att,j} = \prod_{i=1}^{NS} a_i^{\nu_{i,j}} = \prod_{i=1}^{NS} (P * x_i)^{\nu_{i,j}} \tag{2.2}$$

$$K_{eq,j} = K_{att,j} \tag{2.3}$$

2.2. Catalyst preparation

The catalyst preparation started with the synthesis of the porous support CeO_2. Literature reports different paths in order to obtain this type of support with different characteristics [26, 37–39]. Among the others, hydrothermal synthesis method was chosen, because

[1] "i" is the counter for species, "j" is the counter for reactions

it was reported to produce a suitable support for the desired application [26] and because it matched the available instrumentation present in the laboratory where this work was carried out. According to the method, a 8 M solution of $NaOH$ (Sigma-Aldrich) in millipore water was prepared. The highly basic solution was added to 10g of $Ce(NO_3)_3 \cdot 6H_2O$ (Sigma-Aldrich) under stirring until reaching a total volume of 70ml. This mixture was then left under agitation for 30 minutes in order to achieve a homogeneous dispersion. The mixture was transferred into a stainless steel autoclave and left 24h at 100°C. The obtained product was filtered and washed with water and ethanol. The solid particles were dried at 100°C for 2 hours and then calcined at 750°C for 2 hours. One batch was able to produce an amount of CeO_2 close to the theoretical stoichiometric one, thus around 5.5g of support. It is worth to mention that the preparation procedure which was followed from literature did not report any precise amount of chemicals, but similar synthesis methods referred to small amounts of precursor [37]. Because of this, the first synthesis attempt was performed dissolving a very small amount of $Ce(NO_3)_3 \cdot 6H_2O$ (3g) in the volume of solution that could be held by the autoclave capacity (70 ml). Successively the quantity of precursor was increased gradually in order to be able to synthesize enough catalyst in a reasonable amount of time. No change in the mixture pH or other differences were observed while increasing the amount of precursor until the adopted quantity, thus the scale up to 10g of precursor was not considered as an influencing factor for support properties. Many batches have been prepared in order to obtain an amount of precursor sufficient for the experiments and the characterization analyses. However, despite following the same synthesis procedure, significant differences were observed in the product resulting from different batches, in particular in terms of surface area and pore volume (evaluated with BET). For this reason only the batches that matched some specifications were taken into consideration and the final support was obtained by mixing these selected samples in order to obtain averaged homogeneous mixture. The parameters which were taken into account in order to consider the support good enough for the final application were a surface area higher than 20 m^2/g and a pore volume sufficient to impregnate the desired amount of metals. The reason for not obtaining products with constant properties despite following the same procedure could be ascribed to the slight variation of operating conditions during the synthesis process and to the presence of extraneous residues on the employed tools. These impurities might have been present at the time of the project since in the same laboratory other syntheses were being performed. Moreover, it could be the case that a slight change in operating conditions, for example deriving from human error or from instrumentation inaccuracy, could lead to significant differences in the final synthesis result.

The main copper active phase and the metallic promoter Fe were deposited on the cat-

alytic surface by successive incipient wetness impregnation using as precursors $Cu(NO_3)_2 \cdot 3H_2O$ (Sigma-Aldrich) and $Fe(NO_3)_3 \cdot 9H_2O$ (VWR chemicals) respectively. Between the first and second impregnation the catalyst was dried overnight at 100°C. The final product was dried and later calcined at 750°C for 2 hours. Part of the obtained catalyst was collected and in this work it will be addressed as $Cu - Fe/CeO_2$. While the remaining part was split into two batches which were impregnated with two solutions of KNO_3 (Alfa Aesar) with different composition in order to obtain the desired amount of potassium (0.52% and 1.9% respectively). After this step, both K-loaded catalysts were dried at 100°C overnight and calcined at 750°C for 2 hours. The samples obtained in this way will be addressed as $Cu - Fe - 0.5K/CeO_2$ and $Cu - Fe - 1.9K/CeO_2$.
All the obtained catalysts were crushed and sieved in order to obtain an homogeneous particle size distribution, which resulted in particles with diameter below 125 m and a particle size distribution centered around the average value of 70 m. Subsequently the bulk density of the catalytic powder was evaluated using a graduated cylinder. The average density of the powder was 1.873 g/ml.

2.3. Catalyst characterization

In order to characterize the synthesized catalysts and to assess their properties after reaction, different analysis techniques were adopted.

- Catalyst BET surface area and pore volume were evaluated using a "Micrometrics ASAP 2020 surface and porosity analizer".
- To identify the crystalline phases, the samples were characterized with a "PANalytical X'Pert PRO Powder X-ray Diffractometer". The samples where analyzed scanning a range from 5° to 90°, with a scan interval of 0.008°.
- To estimate the actual composition of the catalysts an elemental analysis was performed, by using an ICP-MS technique (Inductively coupled plasma mass spectrometry). The analysis was performed by an external partner, ALS Scandinavia Luleå, Sweden.
- H_2-temperature-programmed reduction (TPR) of catalyst was performed at atmospheric pressure in a conventional flow system "Micrometrics Autochem 2510". The catalysts were placed in a U-shaped tube reactor and, after being flushed with inert gas to remove any residual adsorbed external molecule, were heated in a 5% H_2/Ar stream with a heating rate of 5°C/min, in the range from 100°C to 900°C.

2.4. Experimental setup and analytics

In order to perform the experiments for the evaluation of the catalytic performances of the synthesized catalysts, an experimental setup was specifically built on purpose and a schematic representation is shown in Figure 2.1. The core of the setup is the reactor, which was chosen adopting the typical solution for heterogeneous catalytic reactions, hence a packed bed reactor was arranged by using a quartz glass tube with internal diameter of 8mm, positioned vertically. Despite the reactants for RWGS reaction are H_2 and CO_2, nitrogen was added as inert gas in order to meet the concentration limits of the analysis instruments and to close the mass balance. Thus, the flowrates of the three feed gases were regulated using mass flow controllers (Brooks) which were previously calibrated specifically for the involved gases. The feed lines and the ones connected to analysis instrumentation were made of PTFE flexible pipes, while all the other piping was made of stainless steel pipes. All the utilized piping had an external diameter of 1/4 of inch and all the joints and connections were provided by Swagelok.
Initially the feed gases were mixed adopting two subsequent standard tees, however some mixing problems were observed, probably because of the significantly different flowrates of the three compounds. Because of this, a mixer was introduced. This device simply consists of an expansion chamber which allows the gases to mix more uniformly before being fed to the reactor. The line leaving the mixer was split into two branches, one passing through the reactor, the other bypassing the catalytic bed and going directly to a three way valve to which also the first current joined after passing through the reactor. The three-way valve allowed to select which current to feed to the analysis section, in order to make possible the analysis both of the inlet and of the outlet stream. The analysis of the gaseous streams leaving this three-way valve was performed with a Rosemount NGA 2000 infrared (IR) CO-CO_2 analyzer, which gave a very fast response since it was able to take multiple measurements per second. Moreover, in order to close the mass balance and to measure also the amounts of N_2, H_2, and possible byproducts (in particular methane), a Thermo Scientific C2V-200 Micro GC (micro gas cromatograph) was used as back-end analyzer. The device used three separation columns. The first one was PoraplotU type column, made of Divynilbenzene type U, able to detect CO_2; the second was a Molecular Sieve 5A type column, able to detect CO, CH_4, N_2; the last column contained stationary phase was the same of the second one, but in this case the column was intended to detect H_2. The two former columns used helium as carrier gas while the last one argon. Both the IR analyzer and the GC required the elimination of water from the gaseous stream, because its condensation inside the analytic apparatus would cause damage and measurement errors. For this reason a condenser was placed between the exit of the three way

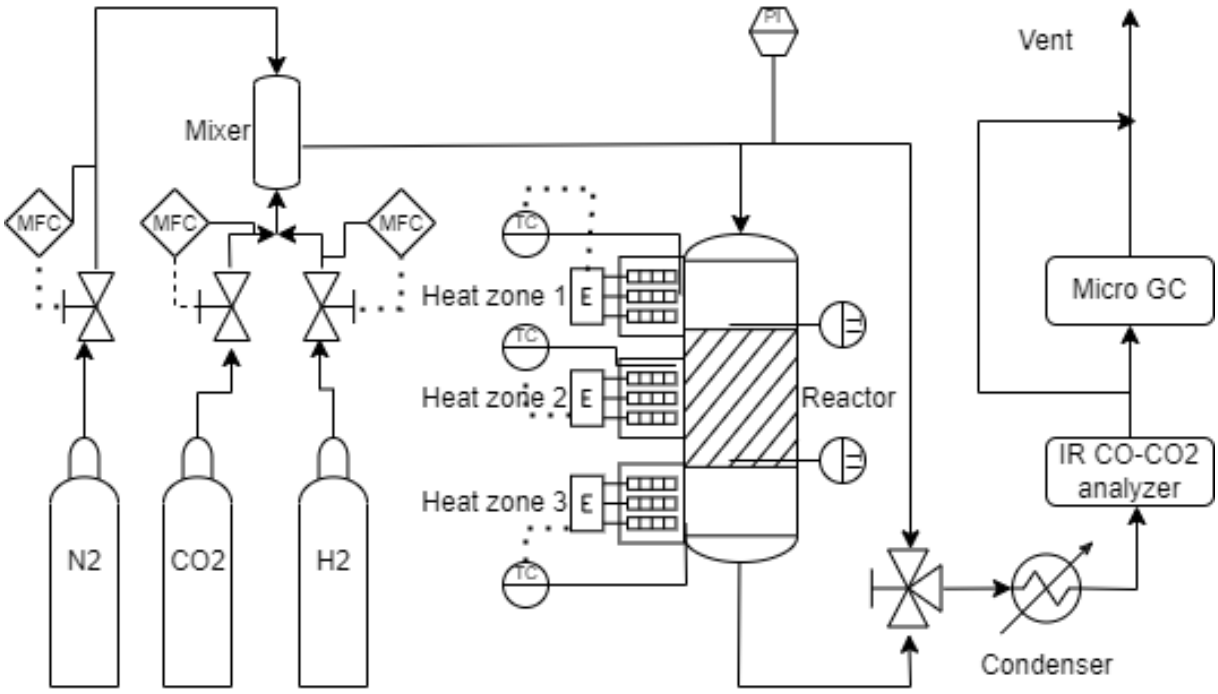

Figure 2.1: Experimental setup

valve and the inlet of the analysis train. The outlet streams were sent to vent.

To provide the heat required by the reaction, the reactor was placed into an oven with three separate heating zones. The whole system until the three way valve, was placed under a fumehood in order to avoid the dispersion in the environment of toxic or hazardous gases. The final section of the setup was not under the fumehood for logistic reasons, and because of this the line which connected the instruments to the fumehood section was periodically inspected for leaks and a portable CO and explosive mixture detector was placed right above this zone.

Regarding the control of the experimental system, as already mentioned, mass flow controllers were adopted to regulate the inlet flowrate of different gases. A manometer was placed before the reactor in order to monitor the pressure drops along the plant. Three different temperature measuring points were present inside the oven, each one connected to a controller for its respective heating zone. In this way it was possible to control the temperature along the length of the unit. Moreover, two thermocouples K-type, were placed inside the reactor, one just above the catalytic bed and the other just in the middle of the quartz wool which was adopted to hold the catalytic bed in position. The temperature of the oven was regulated in such a way that a really small temperature difference (<5°C) could be observed between the top and bottom thermocouple, in this way it was possible to ensure that temperature inside the catalytic bed was reasonably

uniform. An additional thermocouple was applied inside the ending part of the reactor in order to make sure that the o-ring which constituted the sealing between the quartz tube and the metallic junction was never exposed to an excessive temperature which could have caused its melting.
The setup configuration as it has just been described is the result of the resolution of different problems which were faced during construction.The catalytic powder was deposited on a quartz wool bed, which laid on the tip of the bottom thermocouple. A second quartz wool layer was placed on top of the bed in order to keep it in position, even though the gas flow was always downwards. As already mentioned, the measurement of similar temperatures between the top and bottom thermocouple, guaranteed isothermicity in the section included between them, i.e. ensured the isothermicity along the catalytic bed.

2.5. Catalytic runs

In order to establish the performances of the synthesized catalysts, the experimental campaign focused on a temperature interval ranging from 300°C to 700°C (see Section 2.1). The catalyst behavior was evaluated at different temperatures in terms of conversion and selectivity. The lower temperature limit of 300°C has been selected as the minimum value in order to have a sufficient catalytic activity, while the upper limit of 700°C was selected as the maximum reasonable temperature for a realistic application of the RWGS reaction, because the higher is the adopted process temperature, the higher is the external energy requirement. The increase of heat supply demand, indeed, involves lower net CO_2 consumption and higher expenses (see Section 1.5). Hence, each catalyst was tested in this temperature range with steps of 100°C. Furthermore, knowing that the equilibrium conversion is strongly affected by inlet composition, for the $Cu - Fe/CeO_2$ catalyst, different inlet ratios of H_2/CO_2 were tested at every temperature. H_2/CO_2 ratios of 1,2 and 3 on molar basis were selected in order to evaluate the inlet composition effect on the catalytic activity. The expected behaviour is that conversion increases with higher H_2 concentration, but since hydrogen is one of the main issues for the economic and sustainable feasibility of the process (see Section 1.5), a concentration of H_2 three times the one of CO_2 has been selected as an upper reasonable value. Concerning the K-loaded catalysts, only the ratio H_2/CO_2=2 was adopted, considering the general trend with different compositions similar to K-free catalyst. These experiments and were left running for 3 hours until a stable condition was observed. In the end, in order to evaluate the long-term performances of the synthesized catalysts, deactivation tests were performed on the three catalysts at 600°C for 91 hours or more adopting a H_2/CO_2 inlet ratio of 2. For this long tests the temperature value has been selected in order to ensure good

Sample	300°C	400°C	500°C	600°C	700°C	Long run
$Cu-Fe/CeO_2$	1:1,2:1, 3:1	1:1,2:1, 3:1	1:1,2:1, 3:1	1:1,2:1, 3:1	1:1,2:1, 3:1	2:1
$Cu-Fe-0.5K/CeO_2$	2:1	2:1	2:1	2:1	2:1	2:1
$Cu-Fe-1.9K/CeO_2$	2:1	2:1	2:1	2:1	2:1	2:1

Table 2.1: Experimental runs table. For each sample are reported the experiments with temperature and inlet feed composition, to be intended as molar ratio H_2/CO_2

activity while adopting conditions for which literature reports sintering of copper-based catalysts. While the inlet composition was chosen for the same reason exposed concerning the K-loaded catalysts short runs. The experimental runs are summarized in Table 2.1.

All the experimental runs were preceded by the reduction of the catalyst. It was performed at 650°C for 2 hours in a stream with composition 81.25% N_2 and 18.75% H_2. The amount of hydrogen flowed through the catalytic bed was extremely higher with respect to the stoichiometric quantity required to reduce the mass of oxides present, in this way the reduction of species was ensured. The temperature value adopted during reduction was selected considering literature and that the maximum temperature for experiments would have been 700°C, hence a value close to this temperature was preferred, but at the same time from TPR no significant signs of reduction occurred between 650°C and 700°C (see Section 3.2). Thus, the reduction conditions achieved running this step at 650°C would have been similar to the ones obtained at 700°C, but reducing at the lower temperature value applied a reduced thermal stress on the catalyst. Being the temperature effect on catalyst deactivation to be determined and unknown a priori at the time of the experimental campaign, selecting a lower reduction temperature was considered a more cautious solution.
Before running the experiments with catalyst, blank tests were performed. SiC (silicon carbide) powder was used as inert packing material in order to observe the extent of reaction under thermal conditions without any catalytic activity. The inert powder was chosen in such a way that it had similar diameter to the one of the synthesized catalyst. In this way, the same conditions associated to the presence of a packed bed in the middle of the reactor were ensured both for blank and catalytic tests.
The total flowrate of the feed stream was 1600 Nml/min for each run and the amount of inert species was 60 [mol%] of N_2. These numbers were selected in order to meet the specifications of the IR $CO-CO_2$ analyzer, which required a minimum flow in order to give a reliable measurement, and it allowed to measure an amount of CO within the

range 0%-10%. Moreover, the operating ranges of the mass flow controllers had to be taken into account and the feed flowrate was further adjusted. With this conditions, in order to have a gas mass space velocity comparable to the ones reported in literature (in the range 60-300 l/g/h) [15, 28, 32], the mass of catalyst loaded for each run was 0.5g. In particular, with the adopted operating conditions of catalytic mass and total flow, the resulting mass hourly space velocity (mhsv, defined as $\dot{Q}_{tot}/m_{cat}$) was 192 l/g/h and the gas hourly space velocity (ghsv, defined as $\dot{Q}/V_{cat}$) was 359543 h^{-1}. The average contact time of gases with the catalytic bed was 0.01 s. These results are referred to stantard conditions (STP). Furthermore, the diameter of the catalytic particles and the diameter of the tube satisfied the general requirements for the operation of a plug flow pattern which are reported below [40].

- $D_{reactor} > 10D_p$
- $L_{reactor} > 50D_p$

The main parameters considered to assess the catalytic performances were CO_2 conversion and CO selectivity. The expressions for these quantities are reported below[2].

$$X_{CO_2} = \frac{\dot{n}^{in}_{CO_2} - \dot{n}^{out}_{CO_2}}{\dot{n}^{in}_{CO_2}} \tag{2.4}$$

$$S_{CO} = \frac{\dot{n}^{out}_{CO}}{\dot{n}^{in}_{CO_2} - \dot{n}^{out}_{CO_2}} \tag{2.5}$$

[2] $\dot{n}^{in}_i$ is the molar flow of i-th compound at the inlet section, while the superscript "out" refers to the outlet section.

3 | Results and discussion

3.1. Thermodynamic analysis

The results of the thermodynamic analysis of the system are reported in this section. The reactions taken into consideration were:

$$CO_2 + H_2 \leftrightarrow CO + H_2O \qquad \text{R.1}$$
$$CO_2 + 4H_2 \leftrightarrow CH_4 + 2H_2O \qquad \text{R.2}$$

In Figure 3.1(a) the conversion of CO_2 is depicted as a function of temperature for systems with different initial composition. In particular $H_2/CO_2 = 1$, 2 and 3. While in Figure 3.1(b) the effect of temperature and inlet composition on CO selectivity is presented. In the low temperature range conversion slightly decreases, then increases towards higher temperatures, with CO selectivity exhibiting the same trend. This behavior is due to the fact that R.2 is the most preferred reaction until approximately 500°C, hence a temperature increase reduces the equilibrium conversion of CO_2, because it is a strongly exothermic reaction. On the other hand, with a further increase in temperature, the RWGS becomes the most relevant reaction, and we see an increase in conversion, because the main reaction responsible for the CO_2 is now endothermic. This descending-ascending trend is particularly visible for high H_2/CO_2 ratios, for which the methanation reaction at low temperature is strongly favored. Moreover, the general trend regarding different ratios shows higher conversion as the ratio increases, indeed a higher number of hydrogen moles, constitutes an excess of reactant which pushes the equilibrium towards the products for both reactions. On the other hand, higher CO selectivity is observed for lower H_2/CO_2 ratios, because the presence of excess hydrogen in the system increases the overall hydrogenation, favoring methane formation. Furthermore, confirming what observed in the analysis of the equilibrium conversion, the increase of temperature leads to an increase in selectivity towards CO, since R.1 is favored (endothermic reaction). Concluding, at at lower H_2/CO_2 ratios a lower temperature is needed to achieve high CO selectivity.
The effect of pressure on the equilibrium condition is reported in Figure 3.2, where it is possible to observe CO_2 conversion and CO selectivity at a fixed temperature value

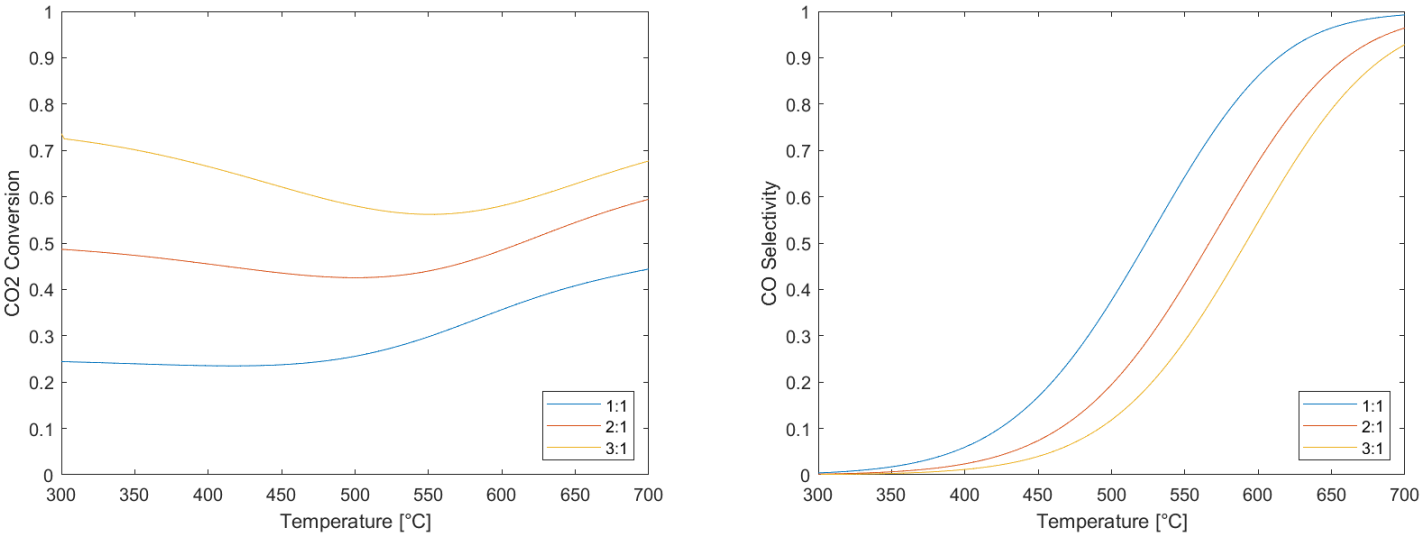

(a) (b)

Figure 3.1: Equilibrium conversion of CO_2 (a) and selectivity towards CO (b) at H_2/CO_2 ratio = 1, 2, 3 as a function of temperature.

(700°C) in the pressure range 1-10 bar. It can be observed that pressure has no significant effect on CO_2 conversion. While selectivity is strongly affected. Indeed, due to the difference in number of moles of the two involved reactions, methanation is strongly favored as pressure increases. Thus CO production is more favorable at low pressure.

3.2. Catalyst characterization

3.2.1. N_2-physisorption

The surface area and pore volume of the pure support and of the synthesized catalysts have been evaluated using the BET method. The adsorption and desorption curves of N_2 at its boiling temperature (77K) are reported in Fig.3.3. All the analyzed samples show a type IV isotherm, typical of mesoporous structures. Moreover, the formation of a hysteresis loop is observed and can be ascribed to the capillary condensation of the adsorbed N_2 molecules inside the structure. The adsorption curve starts to detach from the desorption curve in the range P/P^0=0.65-0.85, while capillary condensation

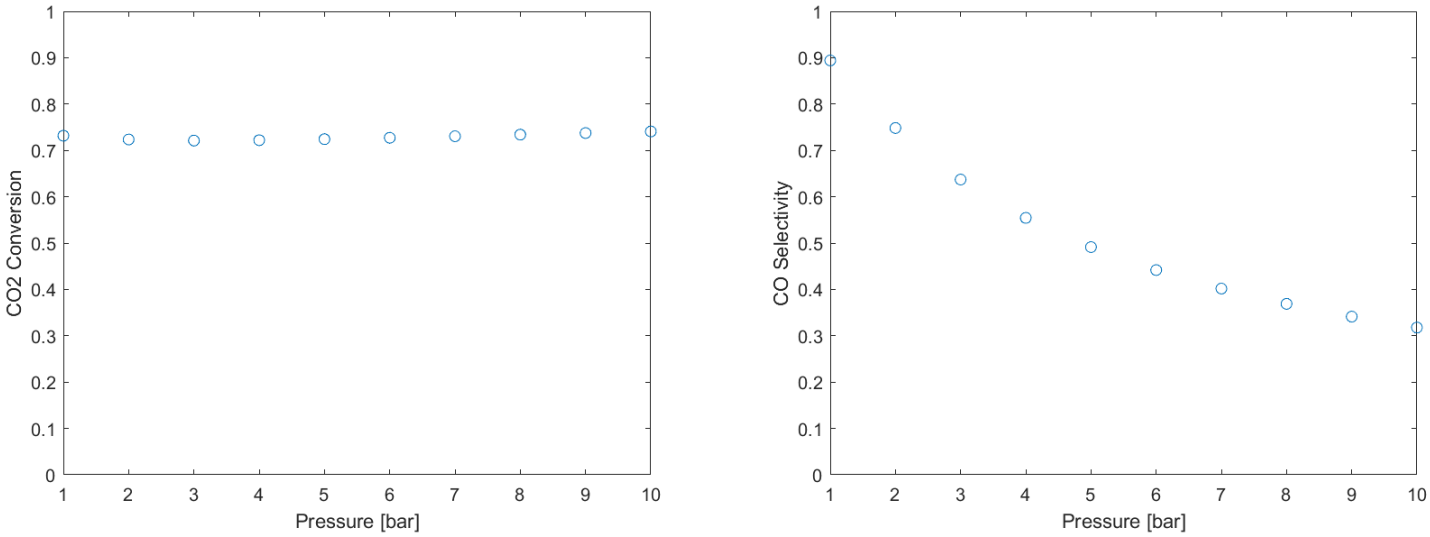

Figure 3.2: Equilibrium conversion of CO_2 (a) and selectivity towards CO (b) at different pressures.

is clear in the range P/P^0=0.85-1. The CeO_2 support obtained as mixture of different synthesis batches presents by far the highest adsorbed volume, followed by $Cu-Fe/CeO_2$, $Cu-Fe-0.5K/CeO_2$, $Cu-Fe-1.9K/CeO_2$. While an opposite trend is observed in the value of relative pressure at which adsorption and desorption curves start to detach. This is was expected since from the first to the last sample the amount of impregnated species increases. Depositing material on the surface reduces the available surface area of the support and partially occupies the pore volume. This result is confirmed by the values of surface area, pore volume and average pore diameter that are reported in Table 3.1. Increasing the amount of deposited metals the surface area decreases significantly from 39.6 to 5.5 m^2/g. The same behavior is observed for pore volume, which undergoes a reduction from 0.29 o 0.059 m^3/g. On the other hand, the average pore size increases following the order $Cu-Fe/CeO_2$, $Cu-Fe-0.5K/CeO_2$, $Cu-Fe-1.9K/CeO_2$, this could be explained considering that the impregnation of material clogs preferentially the smallest pores, thus leaving only the ones with higher diameter. But it is to be observed that the average pore size of the non-impregnated support is slightly higher with respect to $Cu-Fe/CeO_2$. This unexpected behavior might be ascribed to the substantially higher adsorbed volume by the free support with respect to the other samples. Considering that the average pore size diameter is proportional to the ratio between volume and surface

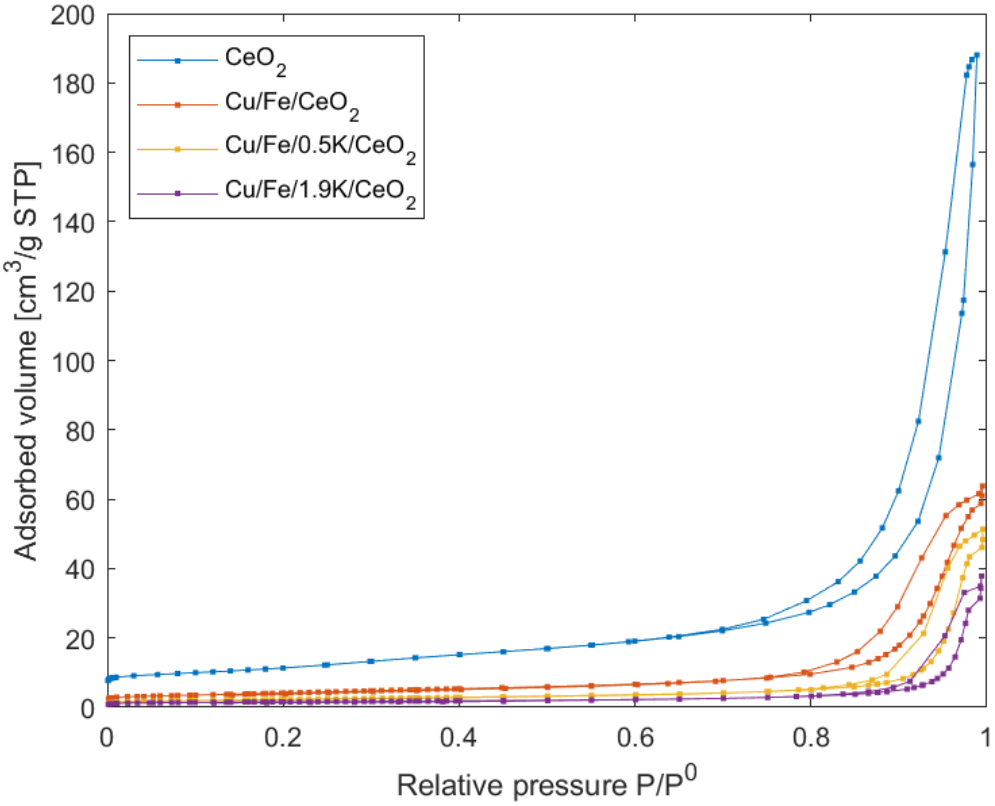

Figure 3.3: N_2 adsorption and desorption curves of liquid nitrogen.

Sample	Surface area $[m^2/g]$	Pore volume $[cm^3/g]$	Average pore size $[nm]$
CeO_2	39.6	0.291	29.5
$Cu-Fe/CeO_2$	14.4	0.099	27.4
$Cu-Fe-0.5K/CeO_2$	7.9	0.079	40.0
$Cu-Fe-1.9K/CeO_2$	5.5	0.059	42.9

Table 3.1: Surface area, pore volume and average pore size of support and impregnated catalysts, obtained with nitrogen adsorption/desorption isotherms.

area, CeO_2 presents a surface area which is almost three times the one of $Cu-Fe/CeO_2$, while the pore volume is around five times, hence a higher pore size is found for the metal oxide free support.

3.2.2. XRD characterization

Figure 3.4 shows the XRD patterns of CeO_2, $Cu-Fe/CeO_2$, $Cu-Fe-0.5K/CeO_2$ and $Cu-Fe-1.9K/CeO_2$. Being ceria the main phase in all the catalysts, it was expected to find the typical nine peaks for this compound (28.546°, 33.080°, 47.482°, 56.341°, 59.088°, 69.413°, 76.699°, 79.074°, 88.427°) (PDF-2 Release 2015 RDB database). These peaks correspond to Cerianite (CeO2). The samples containing deposited metals do not present weakening and broadening of the peaks associated to ceria, hence it can be deduced that the impregnated species do not affect the support crystallinity.
The metallic species deposited on the support are expected to exist under the form of metal oxides, due to the calcination treatment at 750°C in oxidizing atmosphere (air). Some characteristic peaks associated to copper oxide CuO appear in the patterns belonging to copper containing catalysts (35.544°, 38.709°, 48.7°, 61.46°, 66.144°, 68.008°). These peaks are much weaker compared to the ones associated to CeO_2 because copper is loaded on the catalyst low amount (10% in weight) compared to the support. From the obtained patterns no iron crystalline phases could be identified, partly because some peaks associated to iron partially overlap with the peaks for CeO_2 and CuO, but mostly because the iron content is low and might not be detected by the instrument. Moreover it might be below the threshold for crystal detection (typical for XRD = 2 nm), thus the iron particles could be very dispersed.

$Cu-Fe-0.5K/CeO_2$, $Cu-Fe-1.9K/CeO_2$ samples do not show any substantial difference from the K-free $Cu-Fe/CeO_2$, thus it can be stated that similarly to iron

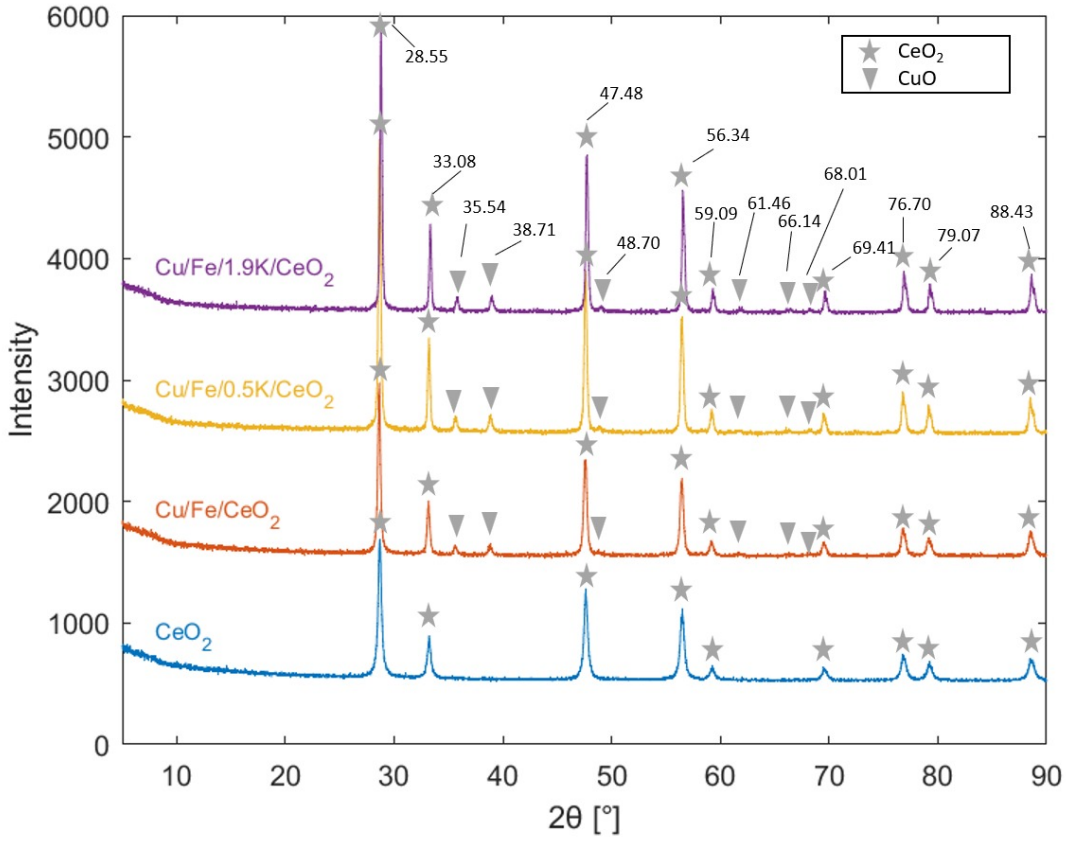

Figure 3.4: XRD diffraction patterns for CeO_2, $Cu - Fe/CeO_2$, $Cu - Fe - 0.5K/CeO_2$, $Cu - Fe - 1.9K/CeO_2$.

species, potassium crystalline phase is not detected because it is present in too low amount and because it is highly dispersed (too small crystals). No peak associated to alloying compounds of Cu and Fe has been detected, indicating that these two species remain independent on the catalytic surface.
To summarize, the results obtained from the XRD analysis suggest that the synthesis procedure succeeded to obtain cerium oxide support with deposited copper oxide. Moreover the addition of this metallic phase to the support seems not to alter the crystalline structure of CeO_2. Futhermore it can be stated that the added Fe and K are highly dispersed on the surface, or at least present in sufficiently low amount to not be detected by the instrument.

3.2.3. ICP-MS

Inductively Coupled Plasma Mass Spectrometry is an elemental analysis able to detect metals and non metals compounds present even at very low concentration. The three samples $Cu-Fe/CeO_2$, $Cu-Fe-0.5K/CeO_2$ and $Cu-Fe-1.9K/CeO_2$ were analyzed with this technique and the obtained results are reported in Table 3.2 in terms of weight percentages.
All samples report an amount of Cu consistent with the aimed loading amount, 11% against the expected 10%. On the other hand a slightly lower amount of Fe is found: 0.42-0.48% against the desired 0.6%. Concerning the amount of impregnated K, significant difference between the aimed and actual loading is observed. Indeed 0.2% of K versus the expected 0.5% is reported in the low K-content sample. While 0.65% versus the expected 1.9% is reported for the high K-content sample. This difference could be due to the saturation of pore volume. Indeed, after the impregnation of Cu and Fe, the available pore volume was quite low (0.099 cm^3/g). Even though this volume was theoretically sufficient to deposit the desired amount of K, during the last impregnation the particles started to agglomerate soon, not allowing for a uniform distribution of the impregnating solution. This premature agglomeration could be due to the non uniformity of the CeO_2 support that was obtained from the mixing of different batches. Possibly the particles with lower pore volume reached the saturation level before the completion of impregnation, hence they started to agglomerate and to hinder the distribution of K solution to the rest of the particles. However, the synthesized catalysts still displayed two different amounts of K promoter, hence the analysis of the results should be interpreted referring to the lower amount of K retrieved in the samples. Anyway the effect of the increasing K loading on $Cu-Fe/CeO_2$ samples can be assessed. Moreover the atomic ratio between K and

Element	$Cu-Fe-CeO_2$	$Cu-Fe-0.5K/CeO_2$	$Cu-Fe-1.9K/CeO_2$
Cerium, Ce	57	56	55
Copper, Cu	11	11	11
Iron, Fe	0.45	0.42	0.48
Potassium, K	0.057	0.2	0.65
Silicon, Si	0.084	0.14	0.078
Aluminum, Al	0.019	0.032	0.023
Calcium, Ca	0.048	0.039	-
Sodium, Na	0.11	0.095	0.14

Table 3.2: Catalyst composition of $Cu-Fe/CeO_2$, $Cu-Fe-0.5K/CeO_2$ and $Cu-Fe-1.9K/CeO_2$ from ICP-MS. All values are expressed in weight percentage. Elements not reported were detected in amount lower than 0.01%.

Cu for the high K-content sample is within the range reported by literature for effective promotion of RWGS reaction [32].
Some unexpected compounds were retrieved, in particular Na is present in significant amount, around 1% in all samples, probably it is a residue from the basic solution utilized during the preparation phase. Si, Al and Ca are present in amount lower than 0.1%, except for Si in $Cu-Fe-0.5K/CeO_2$. These extraneous compounds are probably due to contamination from other preparations which were being performed at the time of this work in the same synthesis laboratory.

3.2.4. H_2-TPR analysis

To investigate the redox properties of the catalysts all samples were subjected to temperature programmed reduction in H_2 atmosphere. Figure 3.5 reports the TPR profiles for the synthesized catalysts. Cerium oxide support presents two clear reduction peaks at 489°C and 795°C. The addition of metals on the catalytic surface causes the loss of the low temperature peak, while the second peak is shifted towards higher temperatures (819°C for $Cu-Fe/CeO_2$, 840°C for $Cu-Fe-0.5K/CeO_2$, 858°C for $Cu-Fe-1.9K/CeO_2$). To explain this, we have to consider that transition metal oxides are reported to have higher tendency to be reduced with respect to ceria, hence they are reduced preferentially. At high temperatures, part of the surface area of cerium oxide is covered by reduced metal oxide species, hence it is less available for reduction itself and the reduction rate is lower. The introduction of Cu and Fe introduces a reduction peak at lower temperature (between 200°C and 250°C), which can be attributed to the reduction of highly dispersed CuO on the catalytic surface [16, 41]. This temperature is lower than reduction temperature of unsupported Cu (ca. 250°C) [42], indicating that high dispersion enhances

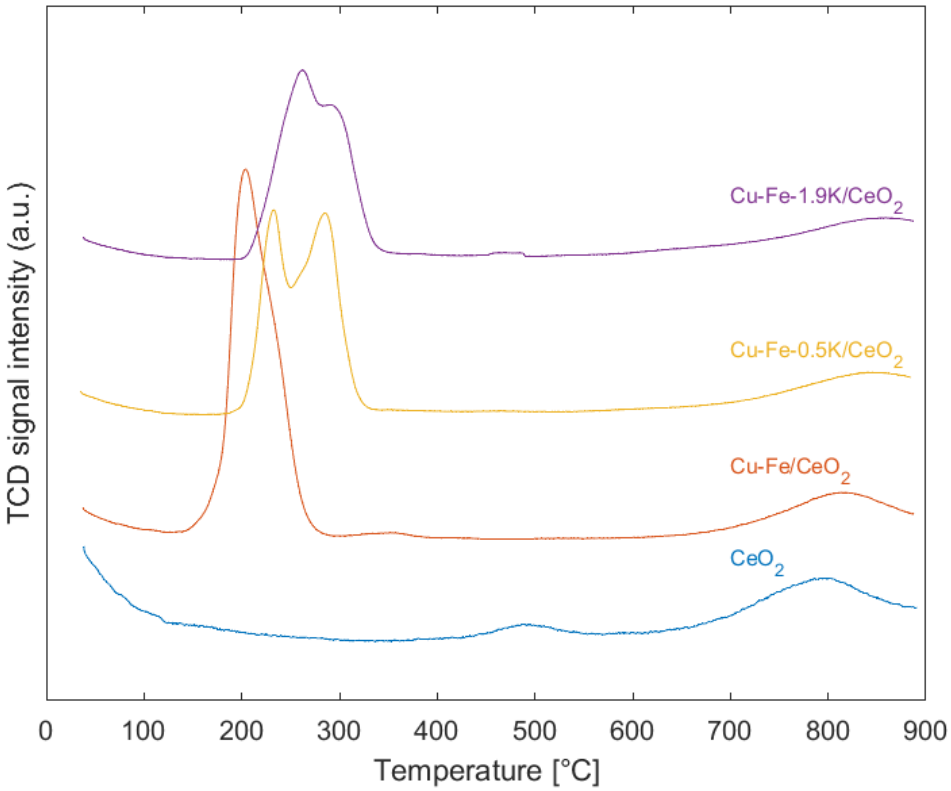

Figure 3.5: H_2-TPR curves for CeO_2, $Cu-Fe/CeO_2$, $Cu-Fe-0.5K/CeO_2$, $Cu-Fe-1.9K/CeO_2$.

the reducibility of Cu species. While no peak associated to CuO included into CeO_2 lattice is observed [16]. Hence no sign of $Cu-Ce$ alloy is identified. This is in agreement with the XRD result, which did not show any defect in ceria lattice after the addition of metal oxides. $Cu-Fe/CeO_2$ presents a weak peak at 352°C, which can be attributed to the reduction of Fe_2O_3 to FeO [43]. The weakness of this peak is due to the small amount of iron loaded, which could also explain its absence in the potassium containing samples. Regarding $Cu-Fe-0.5K/CeO_2$, $Cu-Fe-1.9K/CeO_2$, the peak associated to the reduction of CuO is shifted towards higher temperature, and an other hydrogen consumption peak is detected at 285°C and 292°C respectively. This could be associated to the reduction of potassium phases [44]. It has to be mentioned that a small stepwise bump is present in $Cu-Fe-1.9K/CeO_2$ profile around 500°C. The reason for it is an instrumentation problem encountered while performing the analysis, hence it shouldn't be ascribed to any surface species. The amount of hydrogen consumed during TPR analysis has been calculated by integration of the area under the peaks. From the results reported in Table 3.3 we can observe that below 700°C the overall reducibility of metal

Sample	H2 consumption [STPml/g], (TPR peak position [°C])		
CeO_2	-	12.56(489)	96.86(795)
$Cu-Fe/CeO_2$	84.3(204)	0.763(352)	23.22(819)
$Cu-Fe-0.5K/CeO_2$	51.59(232/285)	-	13.20(840)
$Cu-Fe-1.9K/CeO_2$	49.88(262/292)	-	12.03(858)
$Cu-Fe/CeO_2spent$	6.84(177)	0.759(387)	12.68(859)
$Cu-Fe-0.5K/CeO_2spent$	0.727(176)	1.00(484/520)	10.58(881)
$Cu-Fe-1.9K/CeO_2spent$	4.61(191)	0.498(360)	14.05(865)

Table 3.3: Hydrogen consumption per gram of catalyst with respective reduction peak temperature for CeO_2, $Cu-Fe/CeO_2$, $Cu-Fe-0.5K/CeO_2$, $Cu-Fe-1.9K/CeO_2$ and for three samples $Cu-Fe/CeO_2spent$, $Cu-Fe-0.5K/CeO_2spent$, $Cu-Fe-1.9K/CeO_2spent$ which have been under reacting conditions T=600°C, feed ratio H_2/CO_2=2:1, time on stream larger than 91 hours.

oxides containing samples is significantly higher with respect to free support, the reason could be the excellent reducibility of transition metal oxides [16]. This aspect is particularly visible for K-free samples, where all the deposited copper and iron are available for reduction, while the addition of potassium might cover part of the transition metals surface area, hence a minor reducibility is experienced. An other possible justification for the lower reducibility of potassium-containing catalysts is that K might reduce the oxidation state of surface species by means of $K-Cu$ or $K-Fe$ interaction. Moreover, we have to take into consideration, that the surface area of this samples decreases with the increase of impregnated metals loading, as reported from BET analysis, thus this factor could contribute to the reduction of active surface sites available for reduction. On the other hand, the amount of hydrogen consumed at high temperature is significantly larger for CeO_2, because, as already mentioned, at this temperature, all the metal oxides have already been reduced, and their coverage effect on the surface is significant. Whereas the metal-free support is able to be completely reduced. One of the aims of this work is the investigation of deactivation properties of the synthesized catalysts, in particular in order to assess the effectiveness of K-promotion in limiting coke deposition on the catalytic surface. For this reason TPR analysis has been performed also on the three samples which have been for more than 91 hours under reacting conditions: $Cu-Fe/CeO_2spent$, $Cu-Fe-0.5K/CeO_2spent$, $Cu-Fe-1.9K/CeO_2spent$. Their TPR curves are reported in comparison with the ones of the fresh catalysts in Figure 3.6.

The spent samples present a high temperature reduction peak similar to their respective fresh version in terms of intensity (see Table 3.3) and shifted towards higher temperature

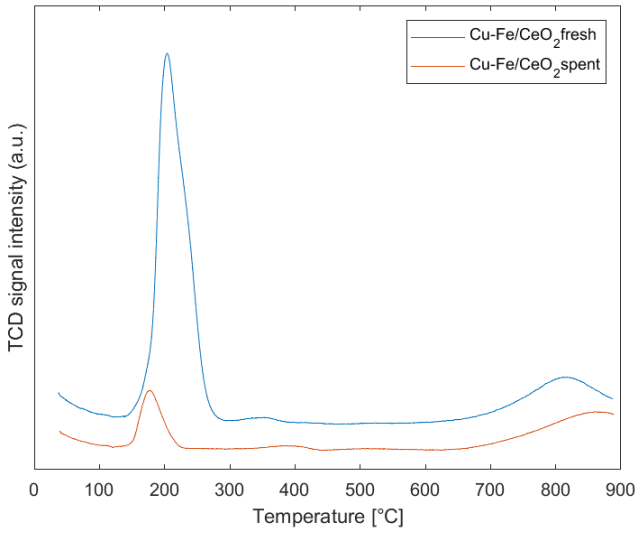

(a)

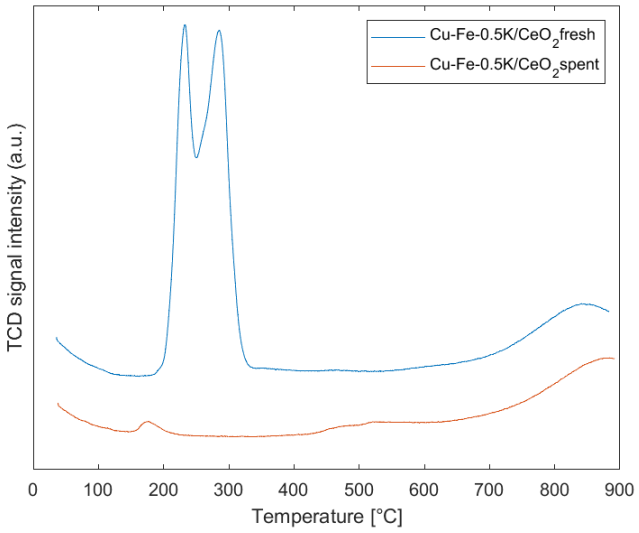

(b)

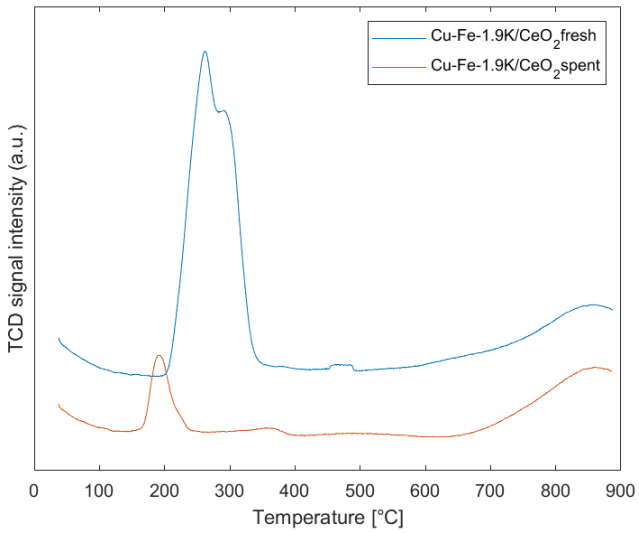

(c)

Figure 3.6: TPR profiles of $Cu - Fe/CeO_2 spent$ (a), $Cu - Fe - 0.5K/CeO_2 spent$ (b), $Cu - Fe - 1.9K/CeO_2 spent$ (c), each one in comparison with their fresh version.

values. Remembering that this peak is associated to reduction of some CeO_2 phase, we can state that support phase remains more or less unchanged with reaction concerning the species reducible in the high temperature range (T>700°C). This result is not surprising since the catalyst does not face such a high temperature either during the reduction or reaction step, hence it was not very likely to experience significant variations before and after the time on stream. On the other hand, the low temperature reduction peaks are much weaker after the reaction, in particular the peak associated to CuO is significantly less intense, while the peaks associated to potassium oxides are not visible at all. Taking into account that the spent catalysts have been reduced at 650° before reacting, the bumps visible on TPR profiles are indicators of surface species that have been reoxidized during the time on stream by the reaction with CO_2, whereas the reducing potential of the chemical system was not sufficient to maintain the surface under a completely reduced state. Considering that the catalytic active phase is constituted by partially reduced metals, it can be assessed that these catalysts are quite effective in remaining in the active state, which means that they are able to perform the cyclic oxidation and reduction of surface species. This is suggested by the significant reduction of hydrogen consumption for the spent catalysts. Moreover, the peaks under investigation, present a shift towards lower temperatures, indicating that after the initial treatment and time on stream the metal oxides reducibility is enhanced, being probably conducive to increased catalytic performances. The characteristics discussed above are particularly evident for $Cu-Fe-0.5K/CeO_2 spent$ sample. Moreover, some small additional reduction peaks in the temperature range 360-520°C are detected, probably ascribed to some species produced on the catalytic surface during the reaction, which is highly probable given the complexity of the chemical system and the high number of phases and species that are involved.

To summarize, the TPR profiles showed that the deposition of metal oxides on the surface increases the reducibility of the catalyst at low temperature. While at high temperature, the shift of the peak associated to CeO_2 towards higher temperatures is evidence of some of interaction between the impregnated metal and the support. Moreover the comparison of fresh and spent samples suggests that the catalysts are able to sustain a partially reduced active state during the time on stream, which allows for a good turnover frequency (TOF) in RWGS reaction.

3.3. Catalytic activity

3.3.1. Catalytic performance with and without K-promotion effect

Figure 3.7 reports the comparison in terms of conversion in the temperature range 300-700°C for the different synthesized catalysts with an inlet H_2/CO_2 of 2. Moreover, in order to make the comparison more complete, also the equilibrium conversion and conversion with inert catalyst (thermally performed reaction) are reported. As expected from the equilibrium behavior, all samples exhibit a conversion enhancement with temperature even at this high gas hourly space velocity. In general, performances start to get closer to equilibrium after 500-600°C. This indicates that lower temperatures are not sufficient to activate the catalytic reaction paths. Moreover it can be noted that above 300°C there is a significant improvement in terms of conversion with respect to the thermal runs, and the higher is the operating temperature, the more this is evident. It is to be mentioned that no data is available for thermal run at 500°C, but it is reasonable to expect CO_2 conversions in the range of 1% between 0.55%(400°C) and 1.26%(600°C). For this reason these two points have been connected with a dashed line.

The three synthesized catalysts have similar behavior at low temperature, while after 400°C, $Cu-Fe/CeO_2$ gives the best result in terms of conversion, followed by $Cu-Fe-0.5K/CeO_2$ and $Cu-Fe-1.9K/CeO_2$. This is probably due to the coverage of the main active species by potassium, which is expected to reduce the overall activity not being really active itself in catalyzing RWGS reaction. This is in agreement with the results of BET analyses, which reported a significant decrease in surface area after the addition of K. On the other hand, the K-promoted catalysts exhibit slightly higher conversion at 300°C and 400°C, indicating that they are more active at lower temperature. Moreover, potassium seems to have a beneficial effect on selectivity. Indeed, as it can be observed in Figure 3.8, especially at low temperatures $Cu-Fe-0.5K/CeO_2$ sample allows for a good selectivity improvement. An outlying behavior for $Cu-Fe-0.5K/CeO_2$ is observed at 700°C, where its selectivity drops to 40%, not following the general expected trend. This result might be due to sintering or some interaction, considering that at such a high temperature CeO_2 can be further reduced [45] (see Section 3.2.4).

In general, it is worth to mention that the data for selectivity at low temperature are not very accurate, since conversion is so small that the variations on inlet and outlet flows due to intrinsic experimental fluctuations, can have a significant impact on selectivity results. All tests between 300°C and 500°C exhibited a closure of the carbon balance above 95%. On the other hand, it has to be reported that at 600°C and 700°C the selectivities for

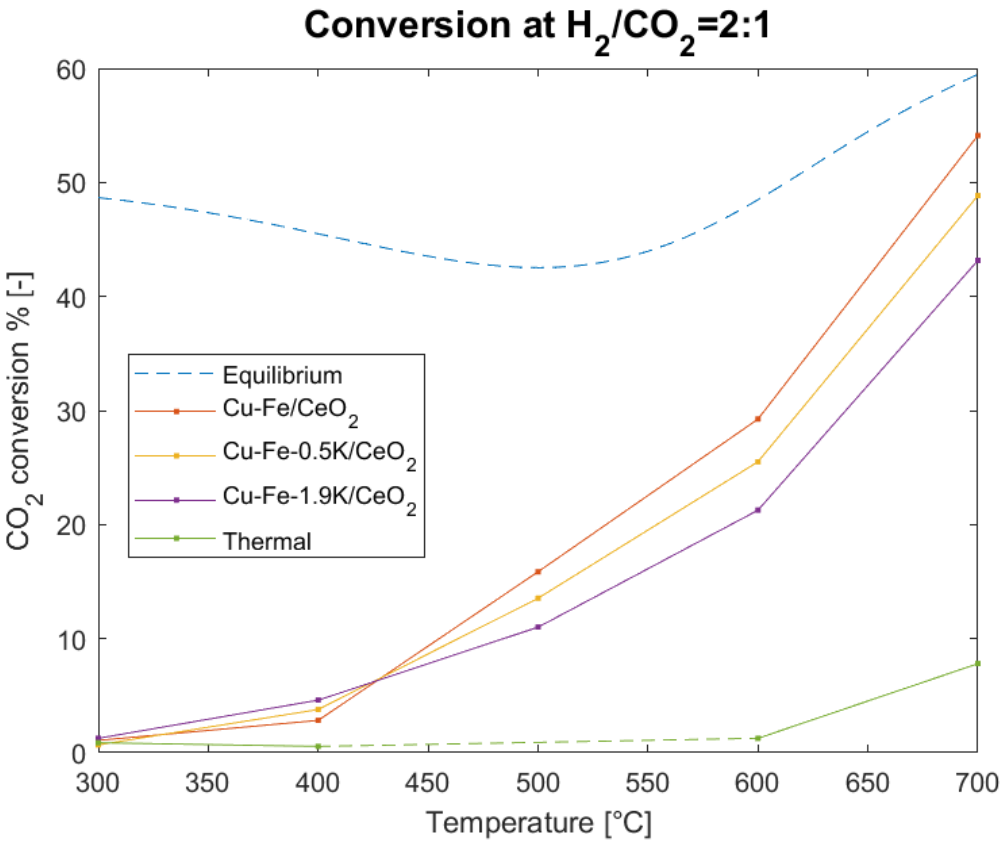

Figure 3.7: Conversion vs temperature for a system at equilibrium conditions for inert catalyst, $Cu - Fe/CeO_2$, $Cu - Fe - 0.5K/CeO_2$, $Cu - Fe - 1.9K/CeO_2$.

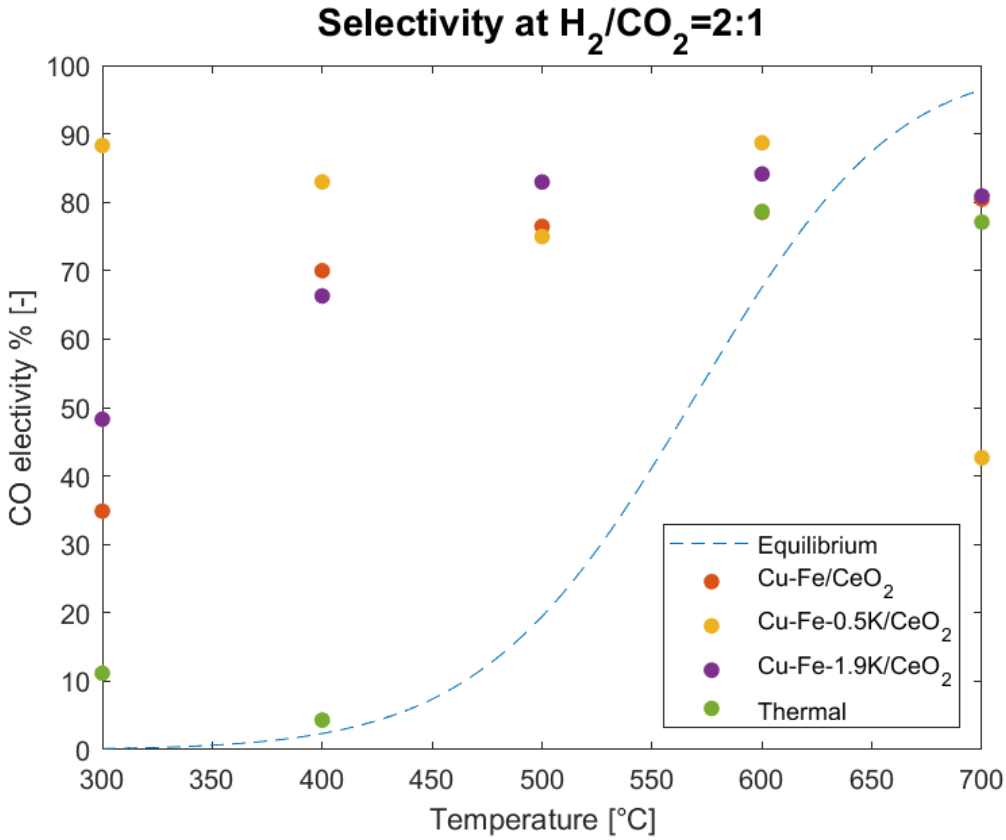

Figure 3.8: Selectivity vs temperature for a system at equilibrium conditions, for inert catalyst, $Cu - Fe/CeO_2$, $Cu - Fe - 0.5K/CeO_2$, $Cu - Fe - 1.9K/CeO_2$.

methane and CO do not add up to 100%. Indeed, selectivity to CO was not 100%, but at the same time the formation of methane was not detected by the micro GC. Considering that no other carbon containing species was detected, the carbon balance was respected in the range from 72% to 97%. To better assess the reliability of the recorded data, the ratio between H_2 and CO_2 consumption on molar basis is reported in Figure 3.9. At low temperature H_2/CO_2 consumption ratio is well above 1. This is an indicator of formation of more hydrogenated species with respect to CO. Thus, in all probability, the formation of some methane takes place, below the detection limit of the GC. From 500°C, the H_2/CO_2 consumption ratio is around 1, indicating that CO is the compound produced in larger amount. $Cu-Fe-0.5K/CeO_2$ at 600°C reports an outlying value that is probably mistaken because the formation of CO is observed (see Figure 3.8), while no H_2 consumption is reported. Since CO formation cannot take place without hydrogen consumption, this datum is to be discarded.
After these considerations, it could be established that the actual selectivity to CO at high temperature (600°C, 700°C), might be higher than what displayed in Figure 3.8, and lower at 300°C and 400°C. The reason for this issue is probably the inaccuracy of the experimental setup and instrumentation. Some inevitable flow fluctuations affect significantly the outlet concentration of compounds present in small amount such as CO, but they do not influence bigger outlet concentrations such as CO_2 and H_2. This explains the discrepancy in selectivity results obtained from CO outlet flow and H_2/CO_2 consumption. Moreover the CH_4 detection by GC was probably not very efficient. An other possibility for discrepancy in selectivity results could be the formation of other species which consume carbon atoms, but the GC did not reveal any additional compound (C_2H_4, C_2H_6, 1-Butene). Given the nature of the chemical system, considering that methanol and higher oxygenates require higher pressure to be formed [10], the only other species that could induce a reduced CO selectivity without CH_4 formation is coke, which remains deposited on the catalytic surface. Even though this is possible, the results of long runs demonstrate that this is very unlikely to happen in the evaluated time scale.

In order to better understand the activity of the various catalysts, Figure 3.10 (a) reports the ratio between obtained conversion and equilibrium conversion and Figure 3.10 (b) reports the ratio between obtained selectivity and equilibrium selectivity. As already observed, at 300°C and 400°C all the catalytic samples are far from the equilibrium conversion, while selectivity is strongly enhanced because no trace of CH_4 has been detected and at low temperature methane is the most favored product at equilibrium. Increasing temperature conversion gets closer to the equilibrium value, up to 91% for $Cu-Fe/CeO_2$, 82% for $Cu-Fe-0.5K/CeO_2$ and 73% for $Cu-Fe-1.9K/CeO_2$ at 700°C. Nontheless good results are achieved even at lower temperatures 500-600°C, which might be more

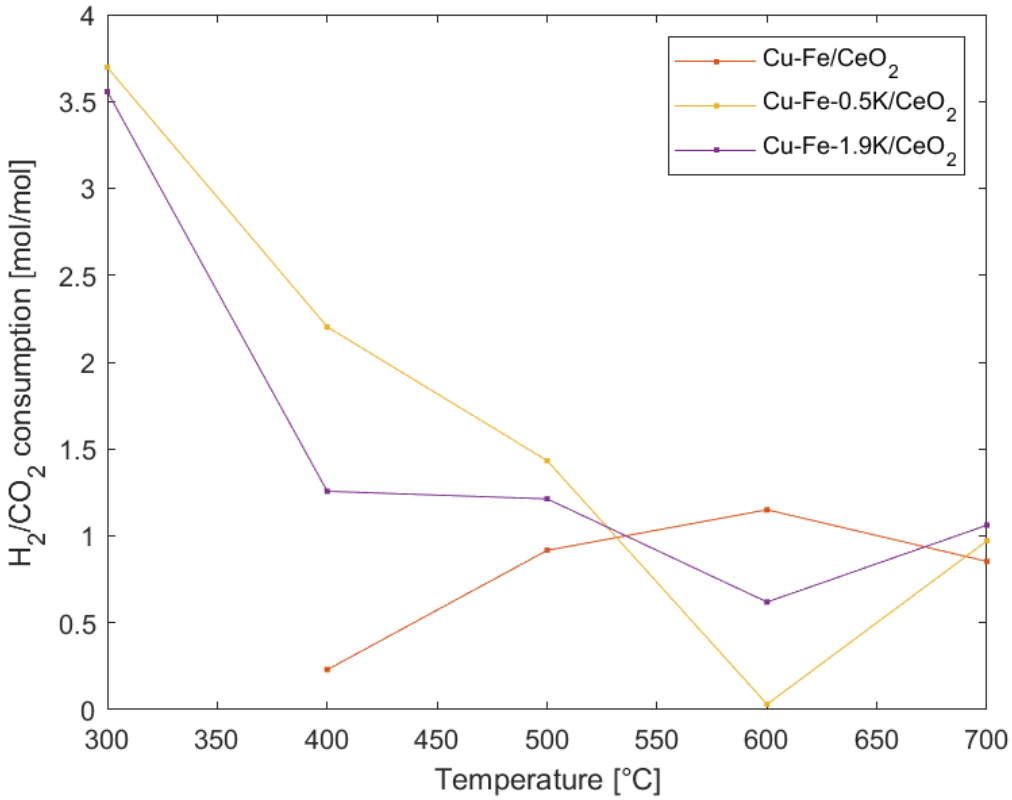

Figure 3.9: Ratio between H_2 and CO_2 consumption on molar basis for $Cu - Fe/CeO_2$,$Cu - Fe - 0.5K/CeO_2$, $Cu - Fe - 1.9K/CeO_2$.

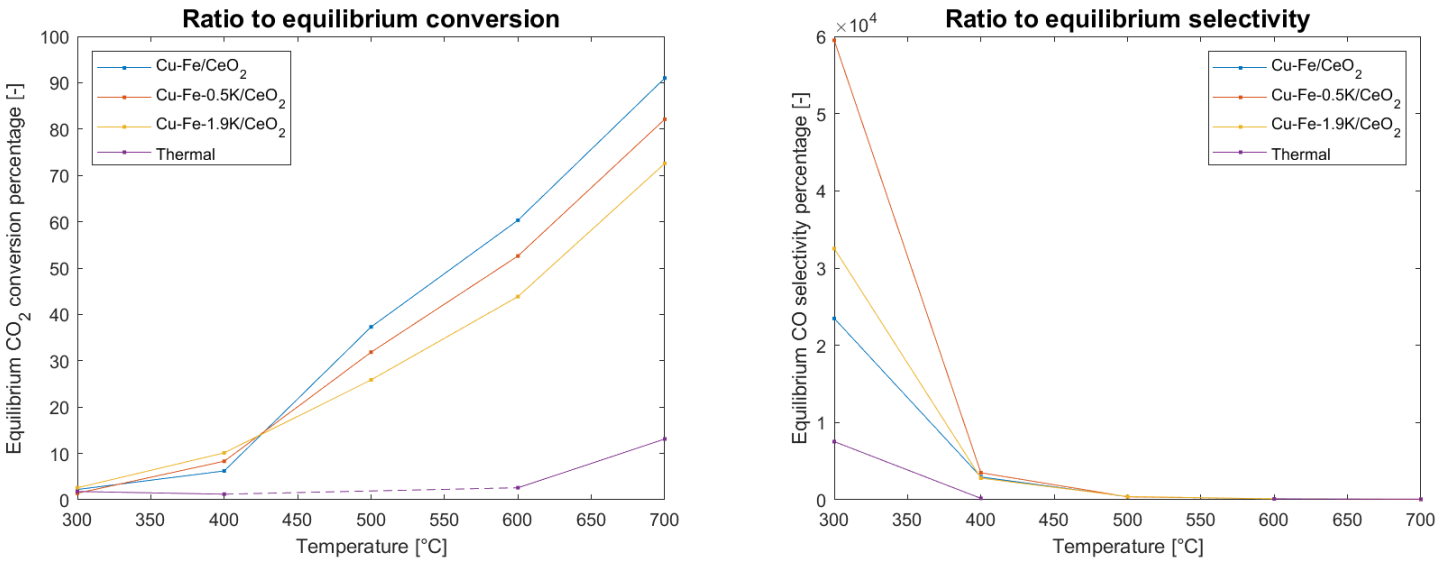

(a) (b)

Figure 3.10: Percent ratio between experimental conversion and equilibrium conversion (a); percent ratio between experimental selectivity and equilibrium selectivity (b) of inert catalyst, $Cu - Fe/CeO_2$, $Cu - Fe - 0.5K/CeO_2$, $Cu - Fe - 1.9K/CeO_2$.

interesting from a feasibility point of view with respect to a higher temperature operation, in order to keep lower the costs and the emissions associated to energy supply. On the other hand, CO selectivity is maintained high while increasing temperature, but also equilibrium selectivity increases to 100%, hence their ratio settles around 1.

In general it can be deduced that the synthesized catalysts are able to perform quite effectively the RWGS at very high space velocity, in particular $Cu - Fe/CeO_2$ gives the best results in term of conversion, while potassium might have a role in enhancing selectivity towards CO especially at low temperature. Hence the K-promotion might be a useful solution for low temperature operation, even though some strategy should be implemented in order to reach sufficient conversion. While focusing on the high temperature range, where conversion reaches higher values, the difference in terms of selectivity is quite negligible between the three samples. In order to establish which would be the most suitable operating condition to perform RWGS reaction, a feasibility study should be performed in order to balance the positive effect of temperature with the cost associated to it. However from this analysis the most active catalyst is $Cu - Fe/CeO_2$.

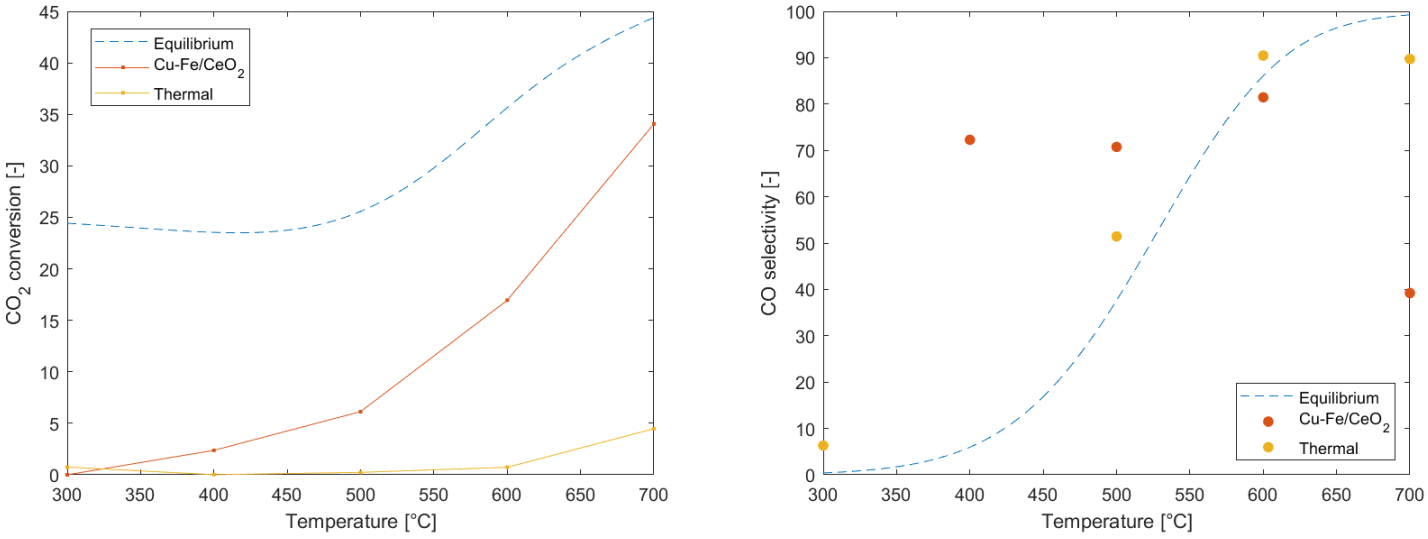

(a) (b)

Figure 3.11: CO_2 conversion of $Cu - Fe/CeO_2$ for H_2/CO_2 inlet ratio=1:1 (a); CO selectivity of $Cu - Fe/CeO_2$ for H_2/CO_2 inlet ratio=1:1 (a).

3.3.2. Effect of inlet H_2/CO_2

Considering that equilibrium conversion increases with the amount of hydrogen present in the feed, $Cu - Fe/CeO_2$ was tested at varying inlet H_2/CO_2 to assess the effect of hydrogen content on catalytic performances. The catalyst underwent three different reacting conditions with molar ratios in the feed equal to 1:1, 2:1, 3:1 (H_2/CO_2). The results of these catalytic tests are reported in Figures 3.11, 3.12, 3.13. In general an increase in conversion with increasing the amount of fed H_2 is noticed. Moreover, for all ratios a conversion enhancement is evident with temperature, thus it follows the trend of equilibrium conditions. Disregarding the hydrogen content present in the feed, temperatures of 300°C and 400°C are not sufficient to promote the catalytic activity at this space velocity, indeed a maximum conversion around just 4% is reached with a 3:1 ratio and the experimental performances are practically unchanged with respect to thermal runs. On the other side, higher temperature allows the activation of $Cu - Fe/CeO_2$, hence the experimental conversion gets closer to the equilibrium value and strongly overcomes the results obtained with thermal runs. Here it has to be mentioned that the data of thermal run at 300°C and 400°C for 3:1 H_2/CO_2 ratio (Figure 3.13 (a)) are not reported because conversion was so small, that the flow fluctuations associated to the practical management of the experimental setup led to non physical results. Indeed, as already mentioned, when

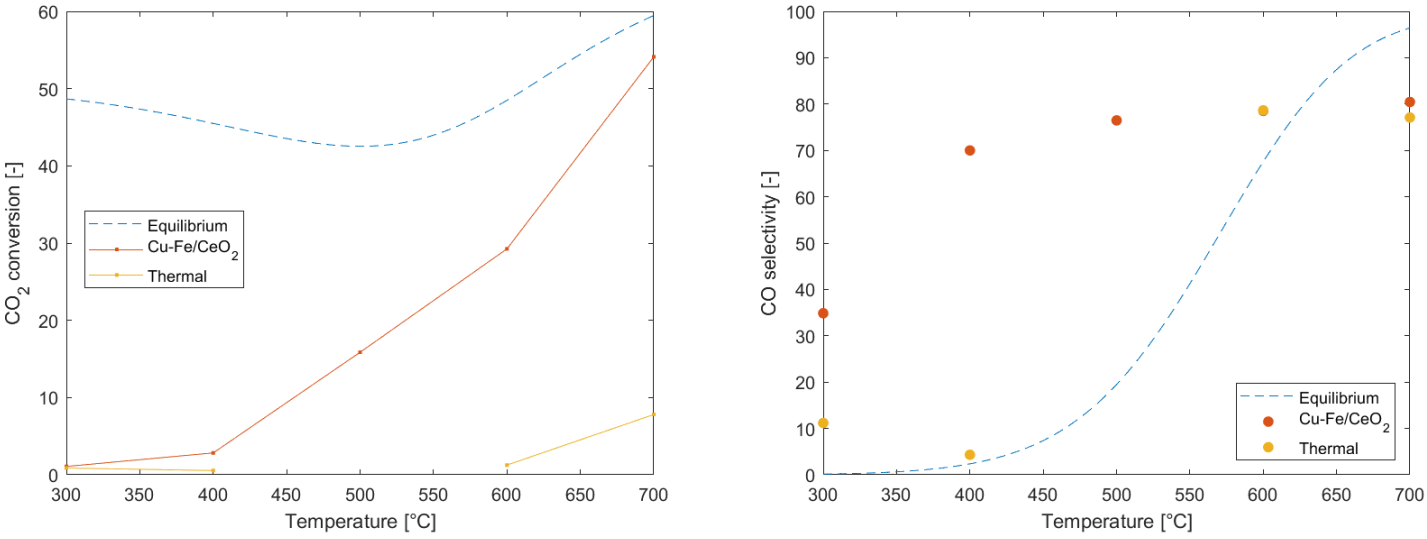

(a) (b)

Figure 3.12: CO_2 conversion of $Cu-Fe/CeO_2$ for H_2/CO_2 inlet ratio=2:1 (a); CO selectivity of $Cu-Fe/CeO_2$ for H_2/CO_2 inlet ratio=2:1 (a).

conversion is very small, the fluctuations may affect significantly the result.
Analyzing more in detail the reported plots, a ratio of 2:1 and 3:1 indicate conversion greater than 15% already at 500°C, while at 600°C they reach 29% and 36% respectively. Nevertheless, at 1:1 H_2/CO_2 ratio, a temperature of 600°C is required to overcome 15% conversion. At 700°C, for all the ratios a remarkable conversion enhancement is observed, in particular approximately a double fold conversion at 600°C is achieved.

Regarding selectivity, at low temperature the catalysts present a scarce selectivity towards CO, despite the uncertainty of the measurements. It is worth mentioning that at 300°C at H_2/CO_2 of 1:1 and 2:1, a selectivity substantially higher with respect to equilibrium value is achieved. This is a consequence of the already reported inaccuracies in selectivity evaluation when CO_2 conversion is very low. It can be deduced that $Cu-Fe/CeO_2$ is able to perform the reaction with significant selectivity towards carbon monoxide from 400°C at H_2/CO_2 ratios of 1:1 and 2:1. Whereas with a higher content of hydrogen in the feed, a temperature of 500°C is required in order to boost selectivity to significantly higher values wit respect to thermal run. This behavior can be explained considering that a higher content of hydrogen penalizes the production of CO as main product due to deeper hydrogenation. However, above 500°C no significant dependence of selectivity on H_2/CO_2 inlet ratio is observed. Moreover, the minimum temperature

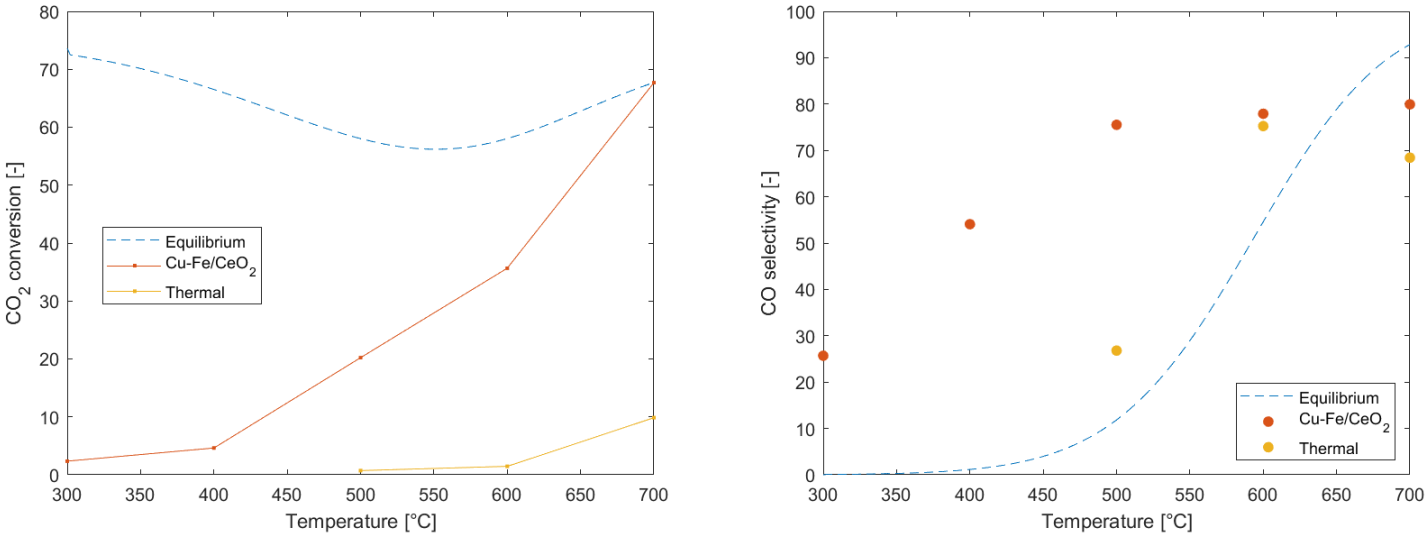

Figure 3.13: CO_2 conversion of $Cu - Fe/CeO_2$ for H_2/CO_2 inlet ratio=3:1 (a); CO selectivity of $Cu - Fe/CeO_2$ for H_2/CO_2 inlet ratio=3:1 (a).

for catalyst activation is in agreement with the results obtained for conversion. In Figure 3.11 (b), it is possible to observe an unusual value for selectivity at 700°C, indeed after remaining above 70% from 400°C to 600°C, it suddenly decreases to 39%.

Since during these tests the same selectivity discrepancy between CO formation and lack of CH_4 was observed, the ratio between H_2 and CO_2 consumption is reported in Figure 3.14. Once again at low temperature we observe a H_2/CO_2 consumption ratio above 1. Even though data at 300°C for inlet ratios 2:1, and 1:1 are not available, it can be expected a lower H_2/CO_2 consumption ratio with respect to the available result for an inlet ratio of 3:1, since theoretically selectivity towards CH_4 is inhibited. On the contrary, at temperatures above 500°C the consumption ratio is around 1. Thus also in this case it should be considered that CO selectivity at low temperature could be lower than what reported in Figures 3.11 (b), 3.12 (b), 3.13 (b). The reason for this discrepancy is the same reported during the analysis of Figure 3.9.

Summarizing the recently made considerations, it is clear that a minimum temperature is required to achieve acceptable CO_2 conversion on $Cu - Fe/CeO_2$ catalyst. In general at 500-600°C it is able to effectively provide good conversion and good selectivity. Of course an operation at 700°C would give better results, but an economic and sustainability evaluation should be made to select the most suitable operating temperature for RWGS.

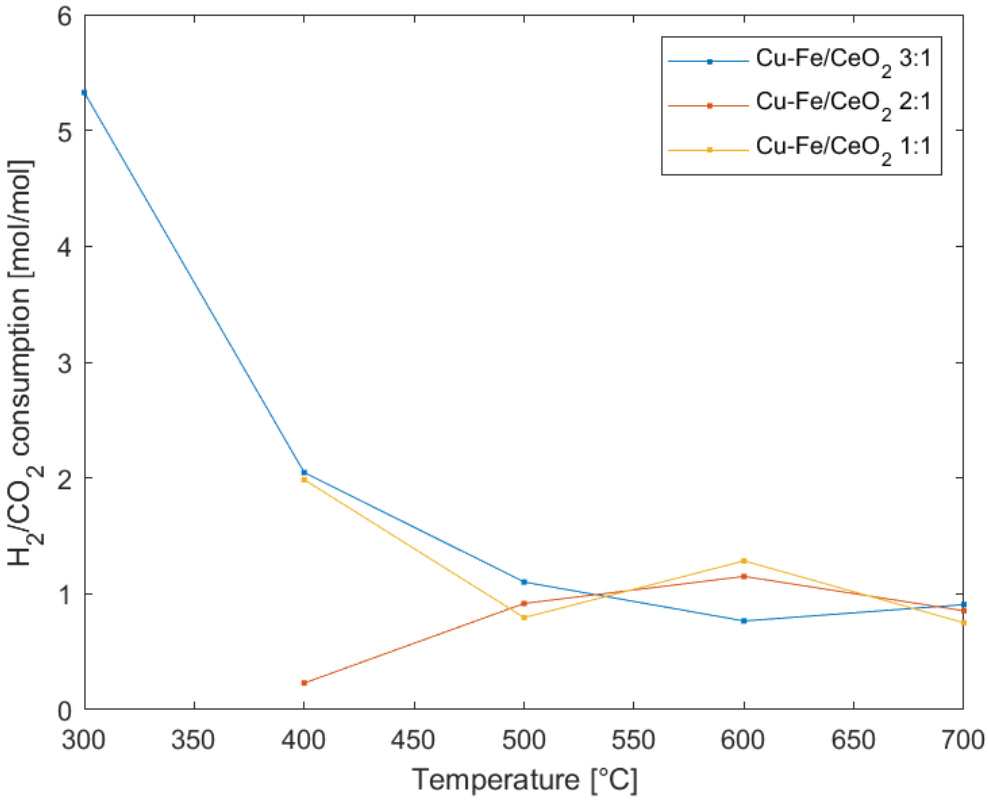

Figure 3.14: Ratio between H_2 and CO_2 consumption on molar basis for $Cu-Fe/CeO_2$ with inlet H_2/CO_2 ratio=1,2,3.

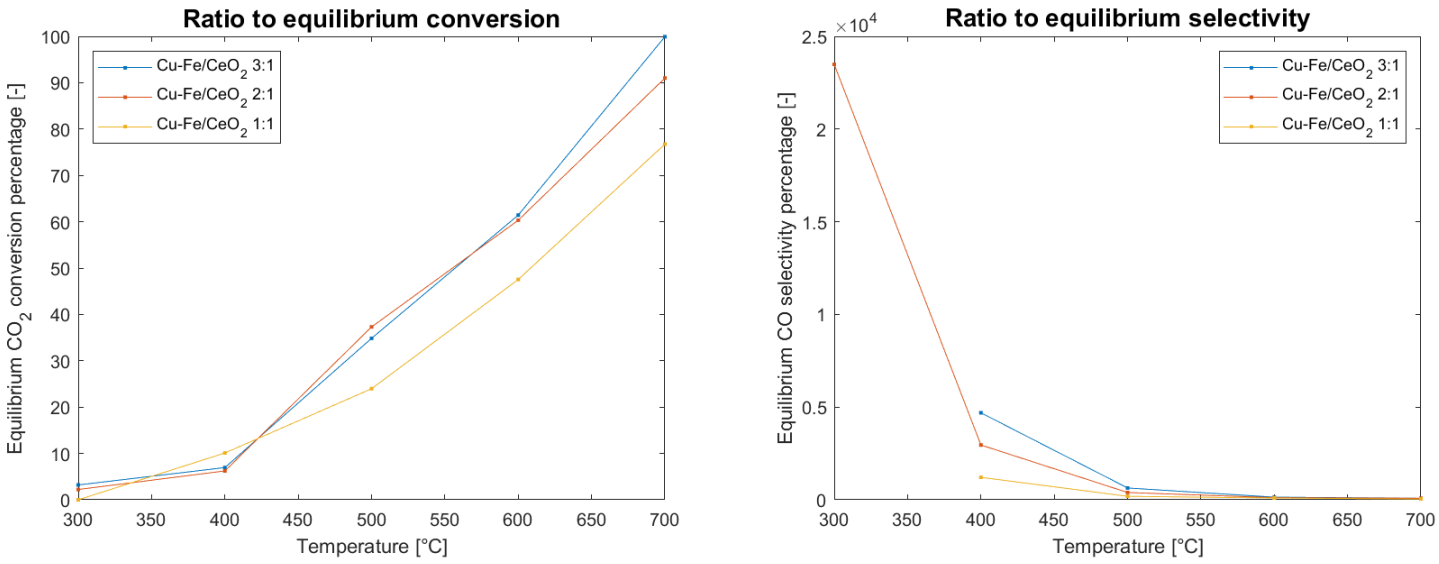

(a) (b)

Figure 3.15: Percent ratio between experimental conversion and equilibrium conversion (a); percent ratio between experimental selectivity and equilibrium selectivity (b) for $Cu - Fe/CeO_2$ at H_2/CO_2 inlet ratio=1:1, 2:, 3:1.

Regarding the amount of hydrogen present in the feed, better performances in terms of conversion are reported with higher H_2/CO_2 ratio, while above 500°C no decrease in selectivity is observed with higher H_2 amounts. Nonetheless, being aware that hydrogen is the main contribution to the reaction cost when blue or green H_2 is used, or it is the main source of CO_2 emissions when grey H_2 is used, it is important to effectively quantify the advantage of using higher amounts of H_2. In order to have a deeper insight on the topic, in Figure 3.15 (a) is reported the percent ratio between experimental and equilibrium conversion, and in Figure 3.15 (b) is reported the percent ratio between experimental and equilibrium selectivity.

In agreement with what already evinced, until 400°C the conversion performances are poor, below 10% of equilibrium value for all the inlet ratios. Increasing temperature, it is possible to notice the detachment of 1:1 curve from the other two. Indeed at 500°C 23.97% is reached with 1:1, while 2:1 and 3:1 report 37% and 35% of the equilibrium conversion respectively. It is interesting to notice that the result for 2:1 and 3:1 ratios is almost the same at 500°C and 600°C. Hence if these were the selected temperatures for RWGS operation, the ratio 3:1 might involve an excessive expense given a limited benefit. Nonetheless, at 700°C an inlet H_2/CO_2 ratio of 3:1 produces a better result with

respect to 2:1, practically reaching the equilibrium conversion value. This result is quite significant considering the relatively large gas hourly space velocity adopted (ca. 360000 h^{-1}). On the other side, a ratio of 2:1 reports a value of 91.00% which is also very high, considering that lower amount of hydrogen is being used. Thus it is not to be excluded that an economical and sustainability analysis identifies an optimal H_2/CO_2 ratio equal to 2:1.
Observing Figure 3.15 (b), it can be deduced that, similarly to what already explained comparing the different K-free and K-containing catalysts, at low temperature the selectivity for all ratios is significantly higher with respect to the equilibrium value. Nevertheless it has to be specified that for inaccuracy problems at low conversions due to flow fluctuations, the selectivity values are not very reliable at 300°C. In general $Cu - Fe/CeO_2$ is able to ensure good CO selectivity at temperatures sufficiently high to allow the proper activation of the catalyst.

3.3.3. Catalyst long term stability performance

The results reported above give a concrete indication about the behavior of the synthesized catalysts under specific reacting conditions. The average test run duration was around 2-3 hours, because this was the amount of time required to reach a steady state trend for outlet concentrations. At first sight, this time lapse was sufficient to develop the catalytic activity and bring the involved surface species to steady state regime, which means, according to the studied chemical system, a steady state regime for redox cycle of surface species (in particular this is the most suitable mechanism for Cu) [19–21]. Even though this condition allows to obtain reliable steady state data, this could be valid only for a limited amount of time. Indeed there may be phenomena that modify the catalyst with very large characteristic time with respect to the few hours required to obtain a preliminary steady state condition. These phenomena could affect the catalytic behavior in the long term, thus their effects are not detectable with a simple short test.
Among the possible modifications that a catalyst could be subjected to, deactivation is a key parameter to be determined. It is the process that causes the deterioration of catalytic performances, reducing the effectiveness in making available an energetically convenient reaction path. Deactivation can be induced by many factors and can follow different mechanisms, depending on the chemical system, operating conditions and type of catalyst [46]. Concerning the catalytic system tested in this study, given the high purity of technical gases adopted (*Linde Gas*), deactivation due to presence of impurities is not to be considered. On the other hand the two most plausible causes for catalyst deactivation

are sintering and coking. The former involves the migration of surface metallic species thanks to high temperature to form less active agglomerates with lower surface area, the latter concerns the formation of carbonaceous deposits (coke) on the surface, which gets progressively covered, reducing the availability of active sites. An other deactivation process that could affect the studied catalysts, is the progressive oxidation of surface species. Indeed the adopted active metals are effective in RWGS catalysis when under a partly reduced state. Which is the reason for the initial reduction that all samples undergo before reacting. The reaction with CO_2 oxidizes the surface and an efficient catalyst should be able to be reduced again back to its original state, guaranteeing a cycle which maintains the catalyst active. Nevertheless this is not always the case, oxidation rate can be higher than reduction rate, thus leading to a progressive deactivation [28]. It is also reported in literature that catalysts involved in CO oxidation containing CuO as surface species might be affected by self poisoning by CO_2, since in the oxidation of CO the desorption of CO_2 is the rate determining step [47]. This poisoning process could affect the catalysts under the present study, but if the surface hydrogenating rate is sufficient CO_2 is rapidly reduced and desorbed in the form of CO.

As already mentioned in Section 1.6, literature reports Cu to be heavily affected by sintering, thus Fe was added in order to limit this deactivation process. Moreover, Fe is preferentially oxidized with respect to Cu and it is more easily reduced [28]. Hence it should provide an improved redox cycle on the catalytic surface, contributing to keep the structure into a reduced state, i.e to keep the catalyst active. The drawback of adopting Fe as active phase is often iron-based catalysts are affected by the deposition of carbonaceous material on the surface [48]. On the other hand potassium is able to promote coke gasification [35, 36]. Therefore, the evaluation of the effectiveness of Fe and K addition in limiting catalytic deactivation has been studied through long runs. The samples $Cu - Fe/CeO_2$ and $Cu - Fe - 0.5K/CeO_2$ were tested, after being reduced with the usual procedure, at 600°C for a time span of 100 and 69 hours respectively. Actually the two samples were analyzed for a similar period of time, but during the experiment with the potassium-containing sample some practical problems invalidated the results, hence reliable data are available only for 69 hours.

Figure 3.16 reports the evolution of CO_2 conversion with time for the two samples under long term investigation. From an overall analysis we can observe that $Cu - Fe/CeO_2$ reaches higher conversion along the whole time range. While $Cu - Fe - 0.5K/CeO_2$ appears less active, confirming what already observed in the short term experiments.

Two step discontinuities are present just before 20 hours of operation and they have opposite effect on the two samples: $Cu - Fe/CeO_2$ conversion increases while $Cu - Fe - 0.5K/CeO_2$ conversion decreases. The reason for these sudden variations is to be found

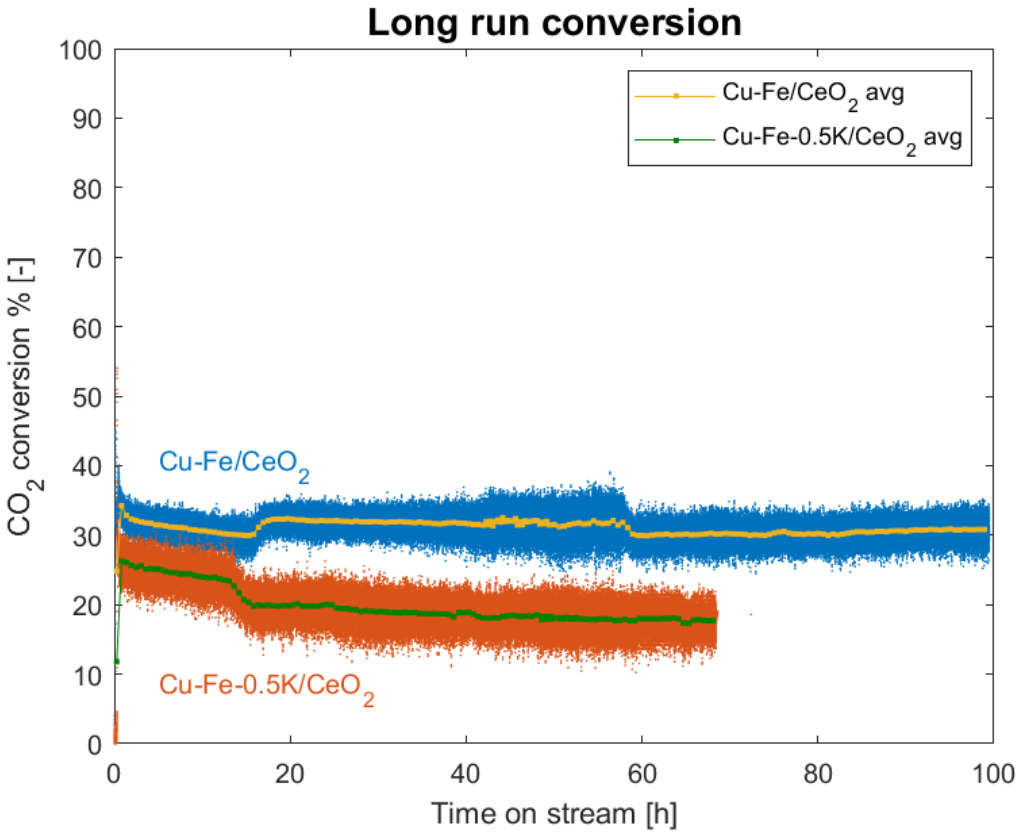

Figure 3.16: CO_2 conversion in time for long term analyses with $Cu - Fe/CeO_2$ and $Cu - Fe - 0.5K/CeO_2$. Both complete and averaged data are reported.

in the operating temperature, which is reported for both samples in Figure 3.17. Indeed, after 18 hours of time on stream a temperature adjustment was required. $Cu-Fe/CeO_2$ was running 5 degrees below the setpoint value, while $Cu-Fe-0.5K/CeO_2$ was running 10-12°C above the setpoint value. Hence, the temperature variations carried out to settle the profiles on their setpoint value explain the corresponding trend observed in conversion profiles. It is interesting to note that the non promoted sample provided higher conversion at the beginning even if it was running at lower temperature by almost 20°C. Thus, it is plausible that potassium, even if present in limited amount, blocks the main sites involved into RWGS reaction, i.e obstructs Cu and Fe particles. The conversion variation after 60 hours on stream in $Cu-Fe/CeO_2$ conversion profile, is ascribed to a minor flow variation in the feed gases.

In order to better understand the trend in time of conversion, Figure 3.16 reports also the averaged trends for both samples. They are obtained taking the average result every 2000 seconds, in this way a smoother line is obtained. With the removal of instantaneous oscillations, it is possible to observe that $Cu-Fe/CeO_2$, after a first settlement, presents an almost steady state average conversion of 30.5% from 25 hours ahead, indeed the yellow line is almost horizontal. On the other hand, not considering the decrease related to temperature variation, $Cu-Fe-0.5K/CeO_2$ shows a decreasing conversion, observable by looking at the slightly negative slope of the green line between 20-69 hours. Even though data after this time are not available, it is reasonable to expect a steady state behavior in the best case scenario, or a continuation of this deactivation trend, following the projection of the green line until 100 hours.

Being the non promoted catalyst able to provide and maintain a better conversion while these advantages are lost in $Cu-Fe-0.5K/CeO_2$, it can be deduced that not only K partially covers the active sites, but it also affects the Fe-Cu interaction. Indeed Fe, added in small amount, forms a matrix which prevents Cu sintering, by keeping the particles in position even at high temperature, while providing an enhanced surface reducibility [28]. At the same time, iron does not affect significantly catalytic performances because it is active towards RWGS reaction and it is able to form some active sites from the interaction with Cu and CeO_2. The unchanged conversion of $Cu-Fe/CeO_2$ in time indicates that Fe is effective in providing the just listed benefits. On the other hand, given the declining performance of $Cu-Fe-0.5K/CeO_2$, it is possible to assess that K has a detrimental effect because it alters the Cu-Fe interaction, indeed its beneficial effect is not observed. Considering the results of TPR (Section 3.2), where all the spent catalysts reported significantly lower hydrogen consumption during the analysis, it was concluded that also the potassium-promoted catalysts were effective in maintaining the catalyst under a reduced state. Hence the deposition of K is not detrimental for the redox catalytic cycle, on the

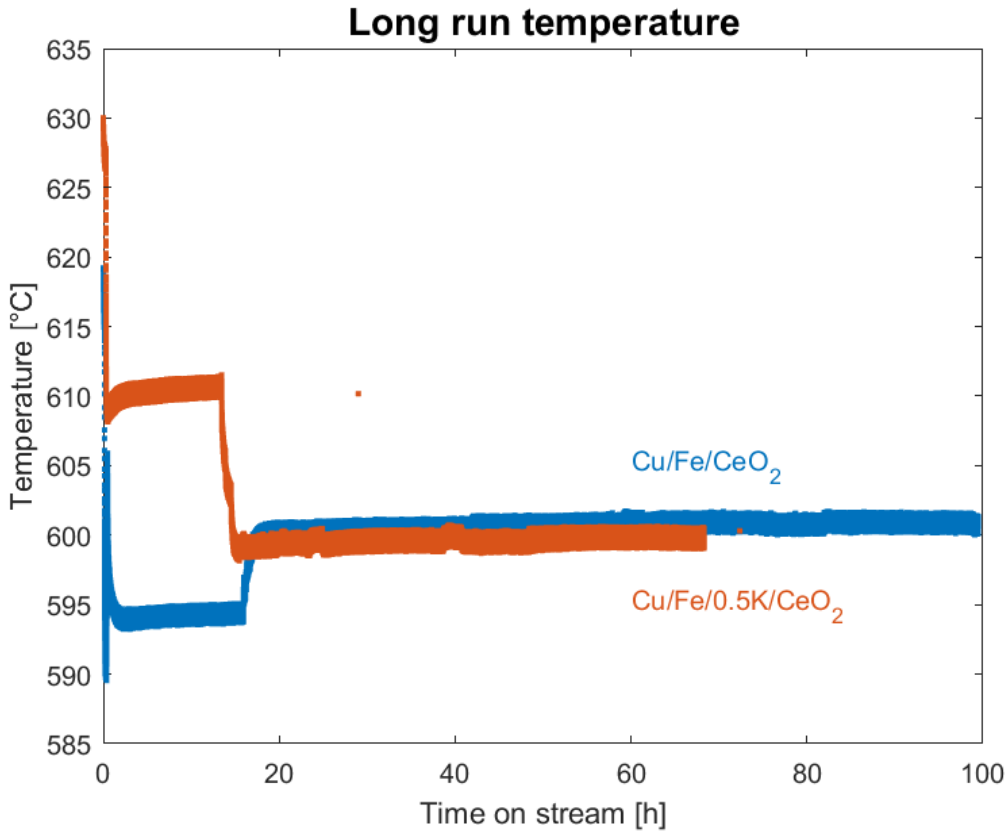

Figure 3.17: Temperature vs time for long term analyses with $Cu - Fe/CeO_2$ and $Cu - Fe - 0.5K/CeO_2$. Temperature values are the average result between temperature above and below the catalytic bed.

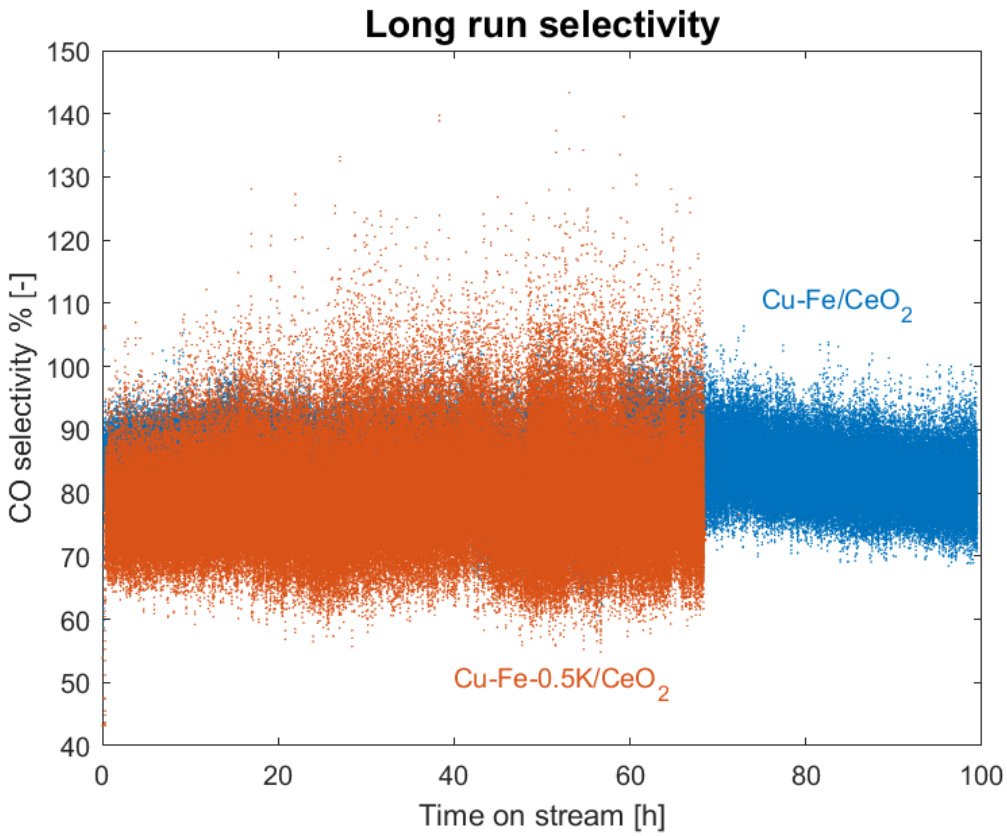

Figure 3.18: CO selectivity in time for long run analyses with $Cu - Fe/CeO_2$ and $Cu - Fe - 0.5K/CeO_2$.

other hand it could weaken the stabilization effect of iron upon sintering, possibly because of some electronic interaction between the surface species. At the same time, not observing an improvement in deactivation prevention with the adoption of K, might be conducive to not consider coking as a relevant phenomenon on this type of catalyst, at least within the range 0-100 hours.

Figure 3.18 reports CO selectivity profiles for the long runs. Despite the heavily oscillating trend, in particular for $Cu - Fe - 0.5K/CeO_2$, it is possible to observe a steady state selectivity around 82% for $Cu - Fe/CeO_2$ and around 80% for the other catalyst. Even though it has to be recalled that no methane formation was measured during these tests. Focusing on $Cu - Fe/CeO_2$, it is possible to notice a small decrease in selectivity around 75 hours, but after 90 hours the profile seems to settle one more time on the horizontal direction. Consequently, the selectivity analysis does not influence significantly the considerations made with the analysis of conversion profiles.

4 | Conclusions and outlook for future work

This work investigated the catalytic activity of a novel bimetallic catalyst for RWGS. The combination of Cu and Fe has been tested on CeO_2, an active support that is capable of participating directly to reaction while interacting with the deposited metals. The promoting effect of potassium was evaluated by means of two different loadings. The catalysts where synthesized, characterized and tested in order to understand their activity, the influence of the inlet H_2/CO_2 ratio and the long term stability performance. The selected catalysts were successfully synthesized and their analysis has produced new insights on the effect of the adopted compounds on RWGS reaction enhancement, since no existing study for catalysts with the same composition has been found at the time of this research.

The experimental setup built on purpose, despite being affected by some inaccuracy problems, allowed for the effective assessment of catalytic performances under the desired reaction conditions.

The three synthesized catalysts require a minimum temperature of 500°C to exhibit a significantly higher activity with respect to thermal reaction. At this temperature they are able to effectively promote the turnover frequency and to give results closer to equilibrium conditions. Optimal performances in terms of conversion are reached at 600°C and 700°C. $Cu-Fe/CeO_2$ proved to be the best performing catalyst, while $Cu-Fe-0.5K/CeO_2$ and $Cu-Fe-1.9K/CeO_2$ suffered the coverage of the active sites by the deposition of K. Indeed their activity decreases with the increase of potassium loading. It is worth to be mentioned that, as expected, the deposition of active species on the catalytic surface reduces significantly the surface area with respect to the free support. The impregnation of K on the already partially covered and clogged catalyst by Cu and Fe, further reduces the available surface area.

The amount of H_2 in the inlet feed affects the outlet results. The higher is the hydrogen concentration, the better is the reproduction of equilibrium conditions, although at 500°C and 600°C, the achieved fraction of equilibrium conversion is the same for H_2/CO_2 ratio of

2:1 and 3:1. Moreover, at 700°C, with an inlet ratio 3:1, $Cu-Fe/CeO_2$ was able to reach the equilibrium conversion, which is quite notable considering the high gas hourly space velocity adopted. On the other hand, selectivity was good for all the synthesized samples provided that temperature was above the activation threshold. Being this condition respected, no difference in CO selectivity was observed depending on the inlet amount of H_2.

The long term runs proved that $Cu-Fe/CeO_2$ is able to maintain the short term performances over a time lapse of 100 hours. Thus it can be concluded that the combination of Cu and Fe as active species is effective for RWGS catalysis. Iron is able to enhance the cyclic oxidation and reduction of copper, avoiding deactivation due to progressive oxidation of the active sites. At the same time, not observing a decay either in conversion or selectivity, establishes that Fe is able to prevent copper sintering. The addition of K does not affect the reducibility enhancement of Cu introduced by iron, but somehow alters the beneficial Cu-Fe interaction. Indeed, during a time on stream of 69 hours a slight deactivation trend is observed, which might be due to sintering. Thus the addition of potassium could alter the electronic surface interactions not allowing for the prevention of Cu particles agglomeration. Moreover, from the comparison between $Cu-Fe/CeO_2$ and $Cu-Fe-0.5K/CeO_2$ during long test runs, it can be deduced that the deposition of carbonaceous structures on the surface does not affect significantly this type of catalysts under the studied reacting conditions. As matter of fact, if coke was deposited on the surface, the gasifying action of K would have inhibited deactivation, while the opposite trend should have been observed for $Cu-Fe/CeO_2$.

The addition of alkali metals was reported to be effective for the enhancement of catalytic properties of Cu-based and Fe-based catalysts for CO_2 hydrogenation [32, 49–51], while this study brings to a different evaluation. The difference between these two conclusions could be justified by considering the nature of the catalytic support. Literature reports a beneficial effect of K addition on SiO_2 support, while this work focused on CeO_2 support. The former is non reducible, while the latter is reducible and actively takes part to the catalytic action. It could be the case that K is able to enhance the performances of Cu on a non reducible support. While, if the support is directly involved into the reaction and it has a strong interaction with the main Cu active phase, K is not able to induce beneficial effects, possibly due to a different nature of surface electronic configuration.

Even though this catalytic system seems promising for CO_2 utilization, to reach a deeper understanding of the chemistry involved and to ultimately design an optimal catalyst for RWGS reaction, there are still many topics to confront.

Despite the general character of this work, it clearly establishes that $Cu-Fe/CeO_2$ is a suitable catalyst for RWGS reaction. Surely future reaserch on the topic will be able

to provide better and optimized solutions, but this result represents a good foundation to develop new technologies following the path marked by Cu-Fe bimetallic catalysts on CeO_2 support.

Therefore catalysts similar to the bimetallic samples synthesized in this study, in particular similar to $Cu - Fe/CeO_2$, could be analyzed more in detail, in order to determine the precise role of the involved species. Consecutively, the understanding of the kinetic mechanism that takes place on this particular catalyst would be of interest. With these information it will be possible to finely tune the catalytic performances by varying the loading of active species. In this way an optimized catalyst could be designed.

Having identified 500-700°C as a temperature range that provides good catalytic activity, it should be investigated more in detail, in order to select the optimal operating temperature. Deactivation effects should be tested over longer periods of time, in order to ensure catalyst durability.

The final goal is the application of RWGS on large scale to effectively reduce the net emissions of CO_2 in the atmosphere, while obtaining the useful product CO. In order to reach this ultimate purpose, a complete feasibility analysis both under the economical and sustainability point of view should be performed, to define the operating conditions that possibly allow for the implementation of RWGS with a positive balance of costs and a net reduction of CO_2.

Bibliography

[1] X. Chen, Y. Chen, C. Song, P. Ji, N. Wang, W. Wang, and L. Cui, "Recent advances in supported metal catalysts and oxide catalysts for the reverse water-gas shift reaction," *Frontiers in Chemistry*, vol. 8, 2020.

[2] R. M. Bown, M. Joyce, Q. Zhang, T. R. Reina, and M. S. Duyar, "Identifying commercial opportunities for the reverse water gas shift reaction," *Energy Technology*, vol. 9, no. 11, p. 2100554.

[3] P. Kaiser, R. Unde, C. Kern, and A. Jess, "Production of liquid hydrocarbons with co2 as carbon source based on reverse water-gas shift and fischer-tropsch synthesis," *Chemie Ingenieur Technik*, vol. 85, no. 4, pp. 489–499.

[4] M. Zhu, Q. Ge, and X. Zhu, "Catalytic reduction of co2 to co via reverse water gas shift reaction: Recent advances in the design of active and selective supported metal catalysts," *Transactions of Tianjin University*, vol. 26, no. 3, p. 172 – 187, 2020.

[5] W. Wang, S. Wang, X. Ma, and J. Gong, "Recent advances in catalytic hydrogenation of carbon dioxide," *Chem. Soc. Rev.*, vol. 40, pp. 3703–3727, 2011.

[6] X. Su, X. Yang, B. Zhao, and Y. Huang, "Designing of highly selective and high-temperature endurable rwgs heterogeneous catalysts: recent advances and the future directions," *Journal of Energy Chemistry*, vol. 26, no. 5, pp. 854–867, 2017. CO2 Capture Storage and Utilization.

[7] R. G. Grim, Z. Huang, M. T. Guarnieri, J. R. Ferrell, L. Tao, and J. A. Schaidle, "Transforming the carbon economy: challenges and opportunities in the convergence of low-cost electricity and reductive co2 utilization," *Energy Environ. Sci.*, vol. 13, pp. 472–494, 2020.

[8] Y. A. Daza and J. N. Kuhn, "Co2 conversion by reverse water gas shift catalysis: comparison of catalysts, mechanisms and their consequences for co2 conversion to liquid fuels," *RSC Adv.*, vol. 6, pp. 49675–49691, 2016.

[9] M. D. Porosoff, B. Yan, and J. G. Chen, "Catalytic reduction of co2 by h2 for synthesis

of co, methanol and hydrocarbons: challenges and opportunities," *Energy Environ. Sci.*, vol. 9, pp. 62–73, 2016.

[10] X. Xiaoding and J. A. Moulijn, "Mitigation of co2 by chemical conversion: plausible chemical reactions and promising products," *Energy & Fuels*, vol. 10, no. 2, pp. 305–325, 1996.

[11] S. Dzuryk and E. Rezaei, "Dimensionless analysis of reverse water gas shift packed-bed membrane reactors," *Chemical Engineering Science*, vol. 250, p. 117377, 2022.

[12] S.-W. Park, O.-S. Joo, K.-D. Jung, H. Kim, and S.-H. Han, "Zno/cr2o3 catalyst for reverse-water-gas-shift reaction of camere process," *Korean Journal of Chemical Engineering*, vol. 17, no. 6, p. 719 – 722, 2000.

[13] C.-S. Chen and W.-H. Cheng, "Study on the mechanism of co formation in reverse water gas shift reaction over cu/sio2 catalyst by pulse reaction, tpd and tpr," *Catalysis Letters*, vol. 83, no. 3-4, p. 121 – 126, 2002.

[14] X. Wang, H. Shi, and J. Szanyi, "Controlling selectivities in co2 reduction through mechanistic understanding," *Nature Communications*, vol. 8, 12 2017.

[15] G. Zhou, F. Xie, L. Deng, G. Zhang, and H. Xie, "Supported mesoporous cu/ceo2-catalyst for co2 reverse water–gas shift reaction to syngas," *International Journal of Hydrogen Energy*, vol. 45, no. 19, pp. 11380–11393, 2020.

[16] B. Dai, G. Zhou, S. Ge, H. Xie, Z. Jiao, G. Zhang, and K. Xiong, "Co2 reverse water-gas shift reaction on mesoporous m-ceo2 catalysts," *The Canadian Journal of Chemical Engineering*, vol. 95, no. 4, pp. 634–642.

[17] J. A. Rodriguez, J. Evans, L. Feria, A. B. Vidal, P. Liu, K. Nakamura, and F. Illas, "Co2 hydrogenation on au/tic, cu/tic, and ni/tic catalysts: Production of co, methanol, and methane," *Journal of Catalysis*.

[18] C.-S. Chen, W.-H. Cheng, and S.-S. Lin, "Mechanism of co formation in reverse water-gas shift reaction over cu/al2o3 catalyst," *Catalysis Letters*, vol. 68, no. 1-2, p. 45 – 48, 2000.

[19] M. González-Castaño, B. Dorneanu, and H. Arellano-García, "The reverse water gas shift reaction: a process systems engineering perspective," *React. Chem. Eng.*, vol. 6, pp. 954–976, 2021.

[20] L. Dietz, S. Piccinin, and M. Maestri, "Mechanistic insights into co2 activation via

reverse water–gas shift on metal surfaces," *The Journal of Physical Chemistry C*, vol. 119, no. 9, pp. 4959–4966, 2015.

[21] H. Jing, Q. Li, J. Wang, D. Liu, and K. Wu, "Theoretical study of the reverse water gas shift reaction on copper modified β-mo2c (001) surfaces," *The Journal of Physical Chemistry C*, vol. 123, no. 2, pp. 1235–1251, 2018.

[22] L. Wang and H. Liu, "Mesoporous co-ceo2 catalyst prepared by colloidal solution combustion method for reverse water-gas shift reaction," *Catalysis Today*, vol. 316, pp. 155–161, 2018. Industrial Catalysis Looks to the Future.

[23] T. Masui, K. Fujiwara, K.-i. Machida, G.-y. Adachi, T. Sakata, and H. Mori, "Characterization of cerium (iv) oxide ultrafine particles prepared using reversed micelles," *Chemistry of Materials*, vol. 9, no. 10, pp. 2197–2204, 1997.

[24] Y.-Q. Su, G.-J. Xia, Y. Qin, S. Ding, and Y.-G. Wang, "Lattice oxygen self-spillover on reducible oxide supported metal cluster: the water–gas shift reaction on cu/ceo2 catalyst," *Chem. Sci.*, vol. 12, pp. 8260–8267, 2021.

[25] S.-C. Yang, S. H. Pang, T. P. Sulmonetti, W.-N. Su, J.-F. Lee, B.-J. Hwang, and C. W. Jones, "Synergy between ceria oxygen vacancies and cu nanoparticles facilitates the catalytic conversion of co2 to co under mild conditions," *ACS Catalysis*, vol. 8, no. 12, p. 12056 – 12066, 2018.

[26] L. Lin, S. Yao, Z. Liu, F. Zhang, N. Li, D. Vovchok, A. Martínez-Arias, R. Castaneda, J. Lin, S. D. Senanayake, D. Su, D. Ma, and J. A. Rodriguez, "In situ characterization of cu/ceo2 nanocatalysts for co2 hydrogenation: Morphological effects of nanostructured ceria on the catalytic activity," *Journal of Physical Chemistry C*, vol. 122, no. 24, p. 12934 – 12943, 2018.

[27] M. Kovacevic, B. L. Mojet, J. G. Van Ommen, and L. Lefferts, "Effects of morphology of cerium oxide catalysts for reverse water gas shift reaction," *Catalysis Letters*, vol. 146, no. 4, p. 770 – 777, 2016.

[28] C.-S. Chen, W.-H. Cheng, and S.-S. Lin, "Study of iron-promoted cu/sio2 catalyst on high temperature reverse water gas shift reaction," *Applied Catalysis A, General.*

[29] C.-S. Chen, W.-H. Cheng, and S.-S. Lin, "Enhanced activity and stability of a cu/sio2 catalyst for the reverse water gas shift reaction by an iron promoter," *Chem. Commun.*, pp. 1770–1771, 2001.

[30] B. Liang, H. Duan, X. Su, X. Chen, Y. Huang, X. Chen, J. J. Delgado, and T. Zhang,

"Promoting role of potassium in the reverse water gas shift reaction on pt/mullite catalyst," *Catalysis Today*, vol. 281, no. P2, pp. 319–326, 2017.

[31] J. L. Santos, L. F. Bobadilla, M. A. Centeno, and J. A. Odriozola, "Operando drifts-ms study of wgs and rwgs reaction on biochar-based pt catalysts: The promotional effect of na," *C*, vol. 4, no. 3, 2018.

[32] C.-S. Chen, W. H. Cheng, and S.-S. Lin, "Study of reverse water gas shift reaction by tpd, tpr and co2 hydrogenation over potassium-promoted cu/sio2 catalyst," *Applied Catalysis A-general*, vol. 238, pp. 55–67, 2003.

[33] M. Gu, S. Dai, R. Qiu, M. E. Ford, C. Cao, I. E. Wachs, and M. Zhu, "Structure–activity relationships of copper- and potassium-modified iron oxide catalysts during reverse water–gas shift reaction," *ACS Catalysis*, vol. 11, no. 20, pp. 12609–12619, 2021.

[34] Y.-X. Wang and G.-C. Wang, "A systematic theoretical study of water gas shift reaction on cu(111) and cu(110): Potassium effect," *ACS Catalysis*, vol. 9, no. 3, p. 2261 – 2274, 2019.

[35] Z. Zhang, Z. Ou, C. Qin, J. Ran, and C. Wu, "Roles of alkali/alkaline earth metals in steam reforming of biomass tar for hydrogen production over perovskite supported ni catalysts," *Fuel*, vol. 257, p. 116032, 2019.

[36] L. Azancot, L. F. Bobadilla, M. A. Centeno, and J. A. Odriozola, "Catalytic reforming of model biomass-derived producer gas," *Fuel*, vol. 320, p. 123843, 2022.

[37] J. Li, Z. Zhang, Z. Tian, X. Zhou, Z. Zheng, Y. Ma, and Y. Qu, "Low pressure induced porous nanorods of ceria with high reducibility and large oxygen storage capacity: synthesis and catalytic applications," *J. Mater. Chem. A*, vol. 2, pp. 16459–16466, 2014.

[38] R. Tang, N. Ullah, Y. Hui, X. Li, and Z. Li, "Enhanced co2 methanation activity over ni/ceo2 catalyst by one-pot method," *Molecular Catalysis*, vol. 508, p. 111602, 2021.

[39] P. Sripada, J. Kimpton, A. Barlow, T. Williams, S. Kandasamy, and S. Bhattacharya, "Investigating the dynamic structural changes on cu/ceo2 catalysts observed during co2 hydrogenation," *Journal of Catalysis*, vol. 381, pp. 415–426, 2020.

[40] C. Perego and S. Peratello, "Experimental methods in catalytic kinetics," *Catalysis Today*, vol. 52, no. 2, pp. 133–145, 1999.

[41] L. Liu, H. Lou, and M. Chen, "Selective hydrogenation of furfural to tetrahydrofurfuryl alcohol over ni/cnts and bimetallic cuni/cnts catalysts," *International Journal of Hydrogen Energy*, vol. 41, no. 33, pp. 14721–14731, 2016.

[42] Z. Yu, L. Zhang, Z. Zhang, S. Zhang, S. Hu, J. Xiang, Y. Wang, Q. Liu, Q. Liu, and X. Hu, "Silica of varied pore sizes as supports of copper catalysts for hydrogenation of furfural and phenolics: Impacts of steric hindrance," *International Journal of Hydrogen Energy*, vol. 45, no. 4, pp. 2720–2728, 2020.

[43] M. Romero-Sáez, D. Divakar, A. Aranzabal, J. González-Velasco, and J. González-Marcos, "Catalytic oxidation of trichloroethylene over fe-zsm-5: Influence of the preparation method on the iron species and the catalytic behavior," *Applied Catalysis B: Environmental*, vol. 180, pp. 210–218, 2016.

[44] K. Pacultová, T. Bílková, A. Klegova, K. Karásková, D. Fridrichová, K. Jirátová, T. Kiška, J. Balabánová, M. Koštejn, A. Kotarba, W. Kaspera, P. Stelmachowski, G. Słowik, and L. Obalová, "Co-mn-al mixed oxides promoted by k for direct no decomposition: Effect of preparation parameters," *Catalysts*, vol. 9, no. 7, 2019.

[45] A. Laachir, V. Perrichon, A. Badri, J. Lamotte, E. Catherine, J. C. Lavalley, J. El Fallah, L. Hilaire, F. Le Normand, E. Quéméré, G. N. Sauvion, and O. Touret, "Reduction of ceo2 by hydrogen. magnetic susceptibility and fourier-transform infrared, ultraviolet and x-ray photoelectron spectroscopy measurements," *J. Chem. Soc., Faraday Trans.*, vol. 87, pp. 1601–1609, 1991.

[46] M. D. Argyle and C. H. Bartholomew, "Heterogeneous catalyst deactivation and regeneration: A review," *Catalysts*, vol. 5, no. 1, pp. 145–269, 2015.

[47] K. Cheng, S. Zhao, J. Ren, H. Li, and Y. Chen, "Co2 self-poisoning and its mitigation in cuo catalyzed co oxidation: Determining and speeding up the rate-determining step," *Catalysts*, vol. 11, no. 6, 2021.

[48] M. Cortazar, J. Alvarez, L. Olazar, L. Santamaria, G. Lopez, H. I. Villafán-Vidales, A. Asueta, and M. Olazar, "Activity and stability of different fe loaded primary catalysts for tar elimination," *Fuel*, vol. 317, p. 123457, 2022.

[49] J. Xu, X. Gong, R. Hu, Z. wen Liu, and Z. tie Liu, "Highly active k-promoted cu/-mo2c catalysts for reverse water gas shift reaction: Effect of potassium," *Molecular Catalysis*, vol. 516, p. 111954, 2021.

[50] I. Shahroudbari, Y. Sarrafi, and Y. Zamani, "Study of carbon dioxide hydrogenation

to hydrocarbons over iron-based catalysts: Synergistic effect," *Catalysis in Industry*, vol. 13, no. 4, pp. 317–324, 2021.

[51] Y. Zheng, C. Xu, X. Zhang, Q. Wu, and J. Liu, "Synergistic effect of alkali na and k promoter on fe-co-cu-al catalysts for co2 hydrogenation to light hydrocarbons," *Catalysts*, vol. 11, no. 6, p. 735, 2021.

A | Appendix A: Temperature and CO_2 molar fraction for all catalytic runs

In order to provide further information about this work, a section of supporting material is reported into this appendix. It contains the temperature and CO_2 profiles of all the short catalytic runs.

A.1. Cu-Fe/CeO_2 at inlet H_2/CO_2=1, 2 and 3

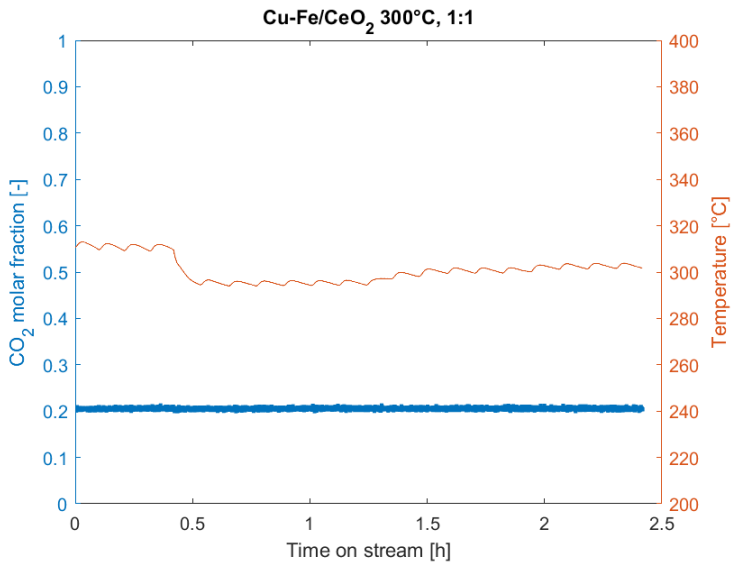

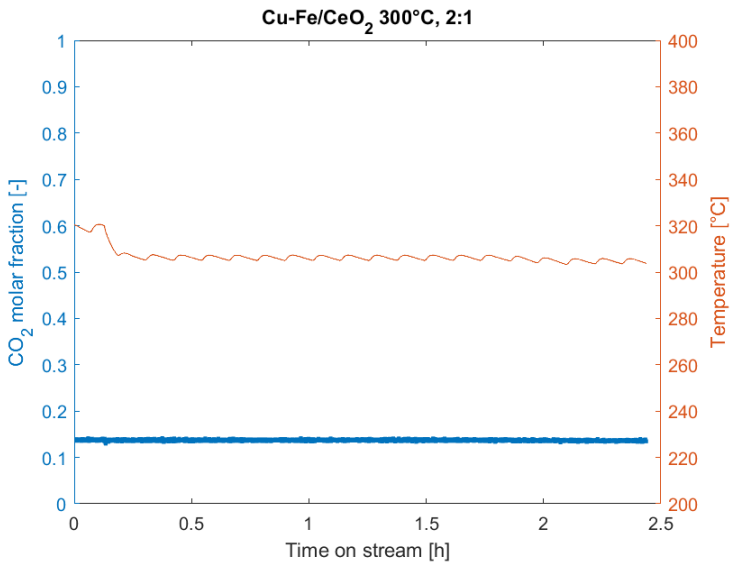

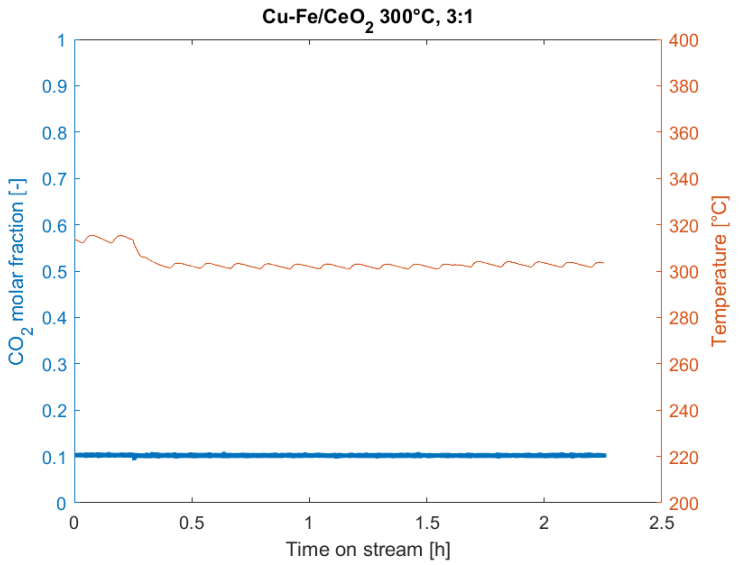
Cu-Fe/CeO2 300°C, 3:1
CO2 molar fraction [-]
Temperature [°C]
Time on stream [h]

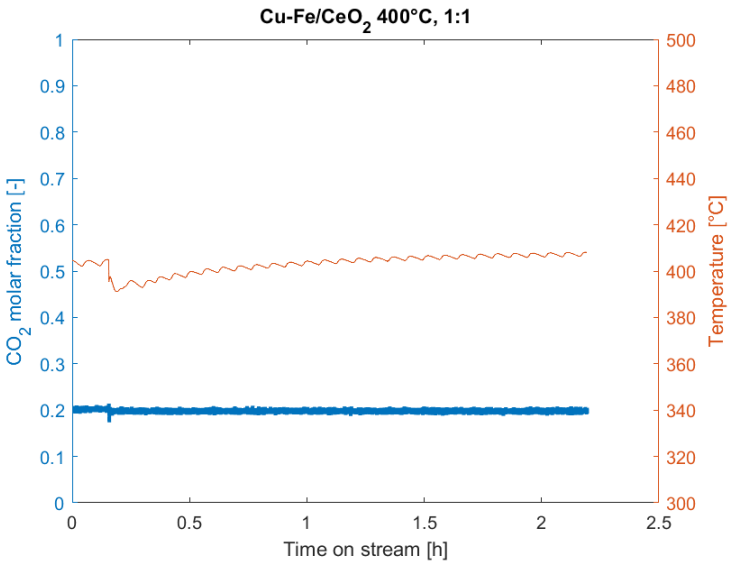
Cu-Fe/CeO2 400°C, 1:1
CO2 molar fraction [-]
Temperature [°C]
Time on stream [h]

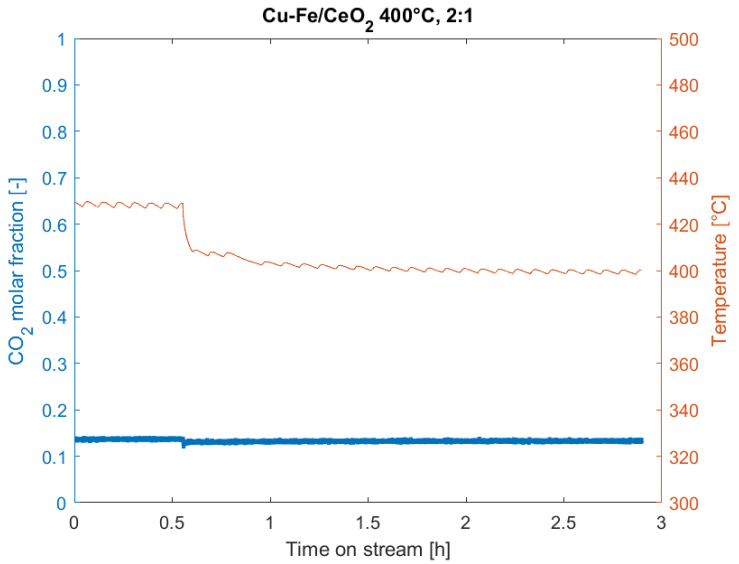
Cu-Fe/CeO2 400°C, 2:1
CO2 molar fraction [-]
Temperature [°C]
Time on stream [h]

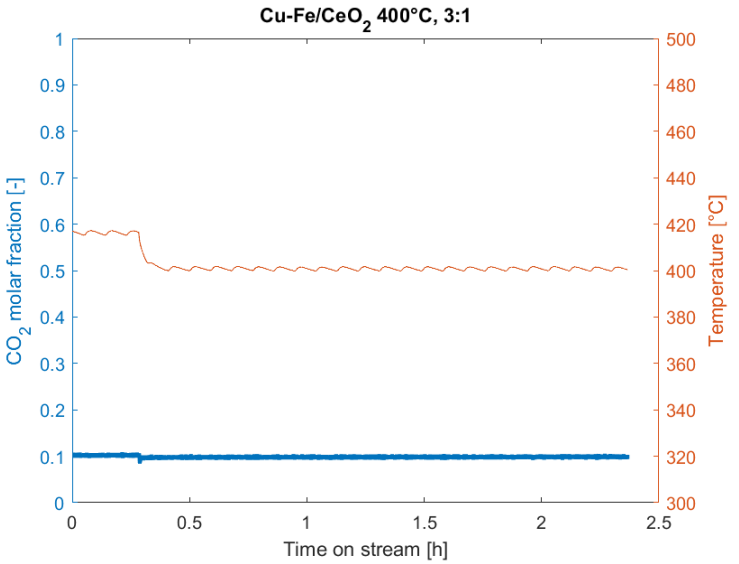
Cu-Fe/CeO2 400°C, 3:1
CO2 molar fraction [-]
Temperature [°C]
Time on stream [h]

A| Appendix A: Temperature and CO_2 molar fraction for all catalytic runs65

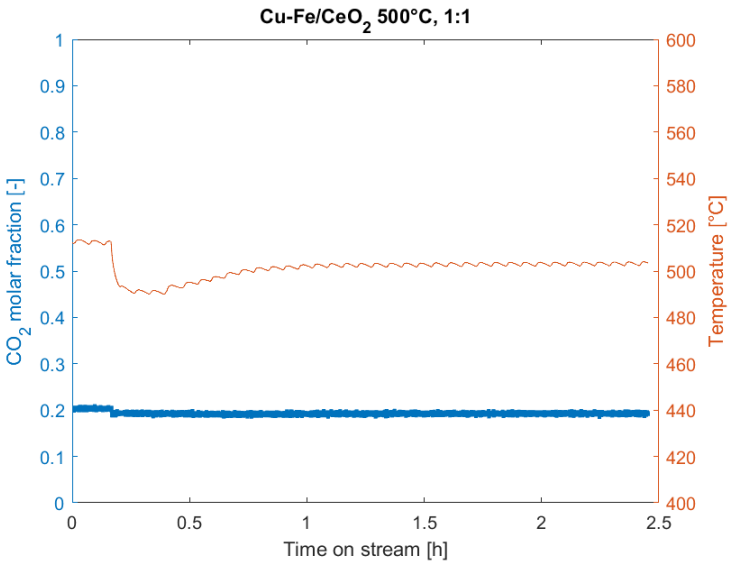

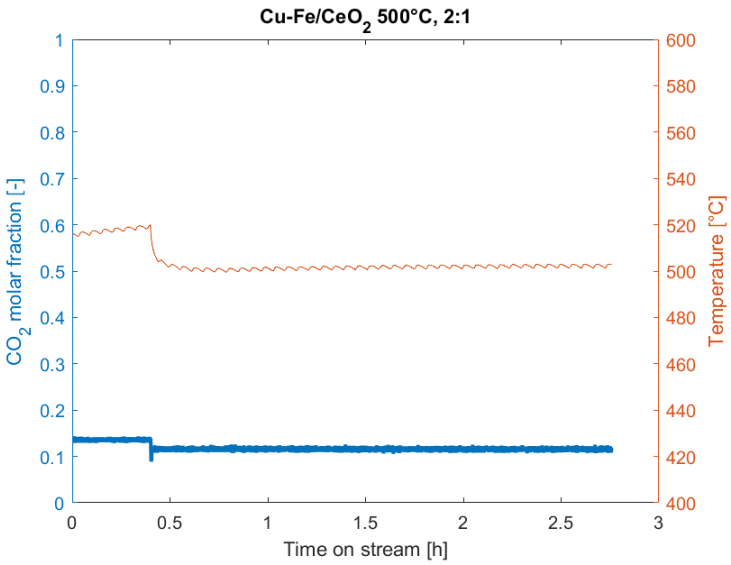

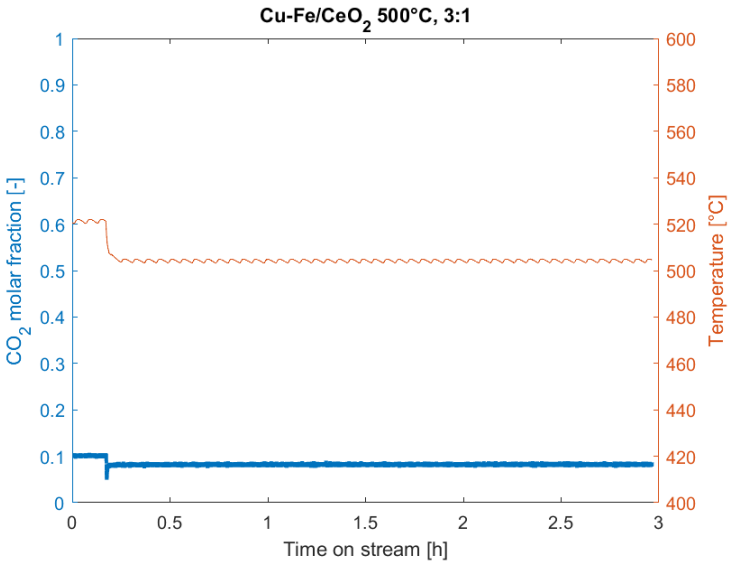

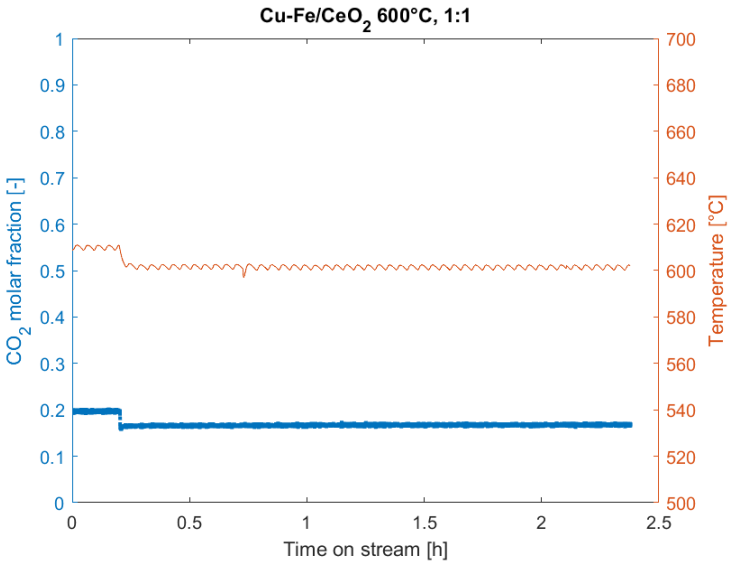

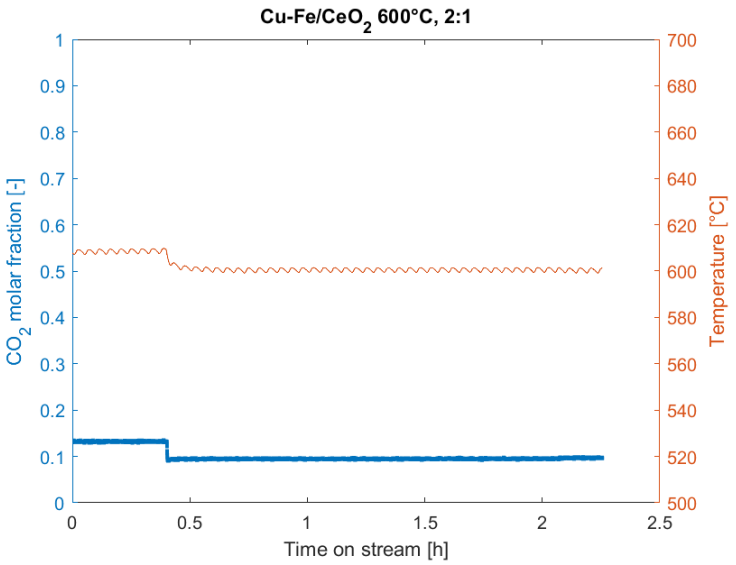
Cu-Fe/CeO2 600°C, 2:1
CO2 molar fraction [-]
Temperature [°C]
Time on stream [h]

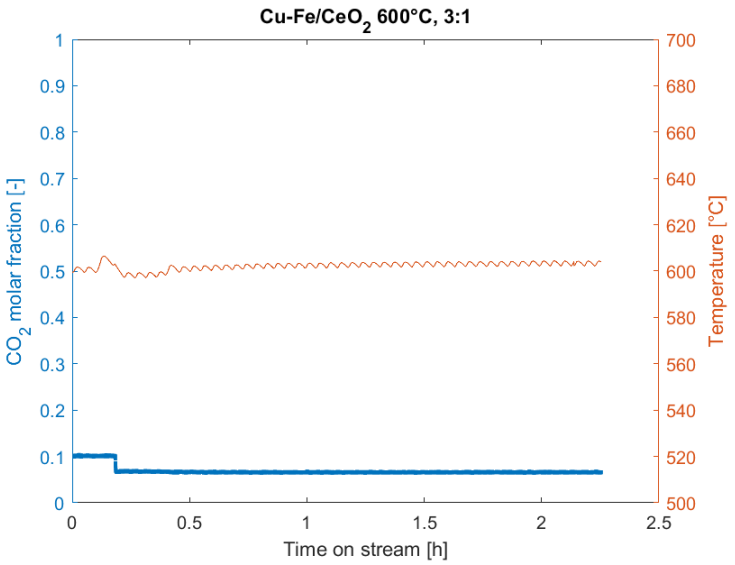
Cu-Fe/CeO2 600°C, 3:1
CO2 molar fraction [-]
Temperature [°C]
Time on stream [h]

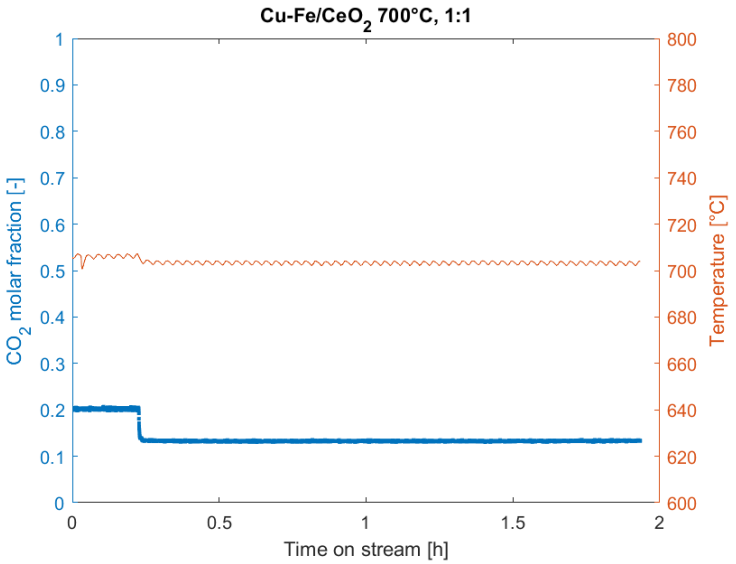
Cu-Fe/CeO2 700°C, 1:1
CO2 molar fraction [-]
Temperature [°C]
Time on stream [h]

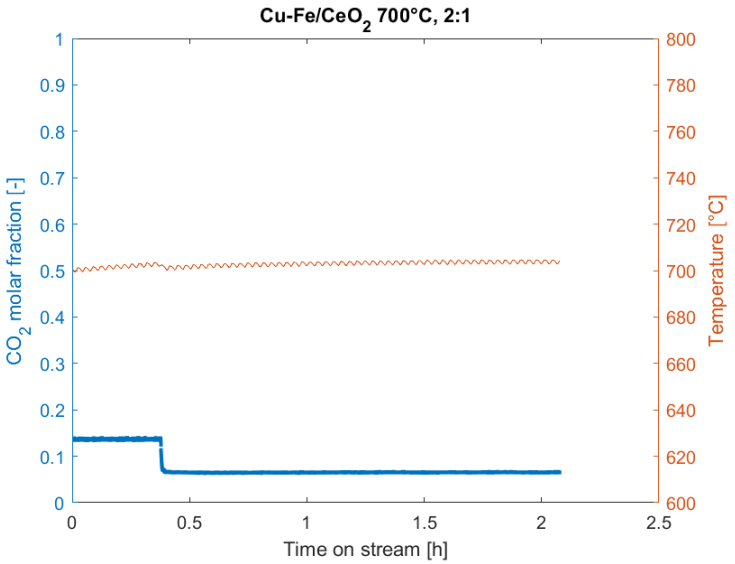
Cu-Fe/CeO2 700°C, 2:1
CO2 molar fraction [-]
Temperature [°C]
Time on stream [h]

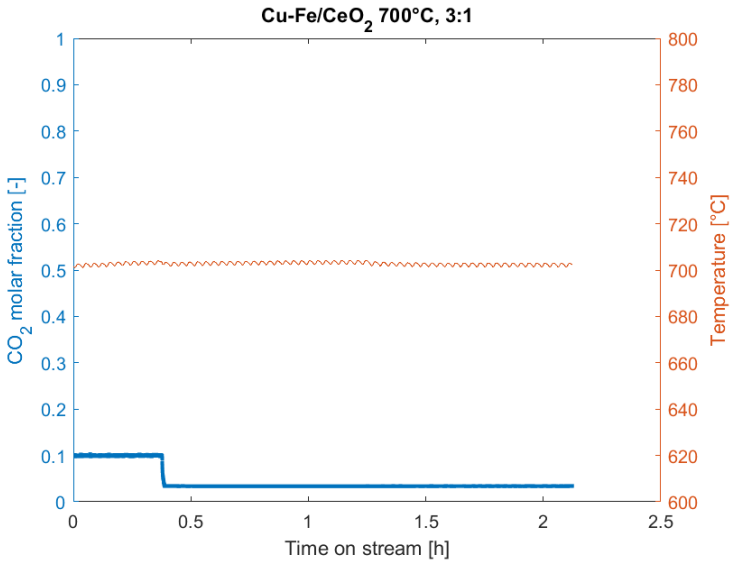

A.2. Cu-Fe-0.5K/CeO_2

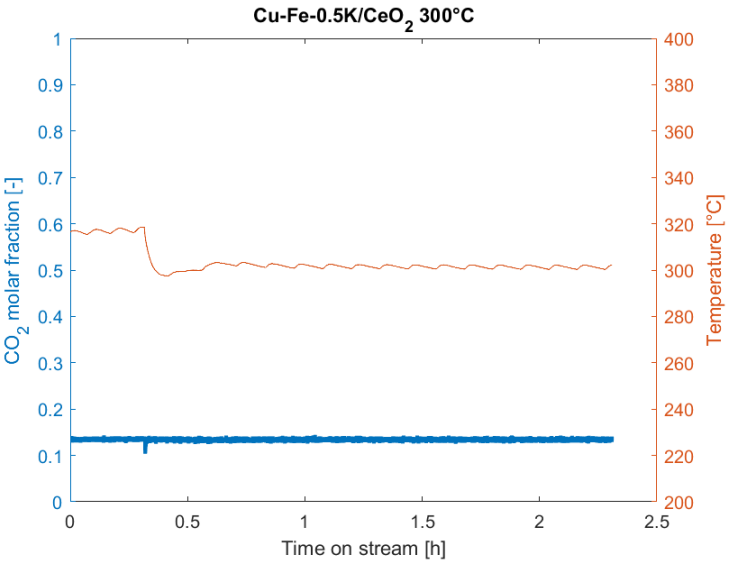

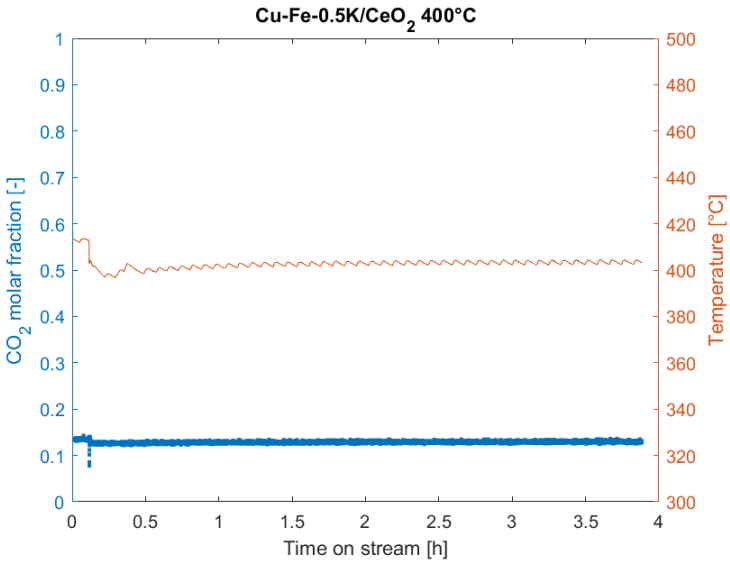

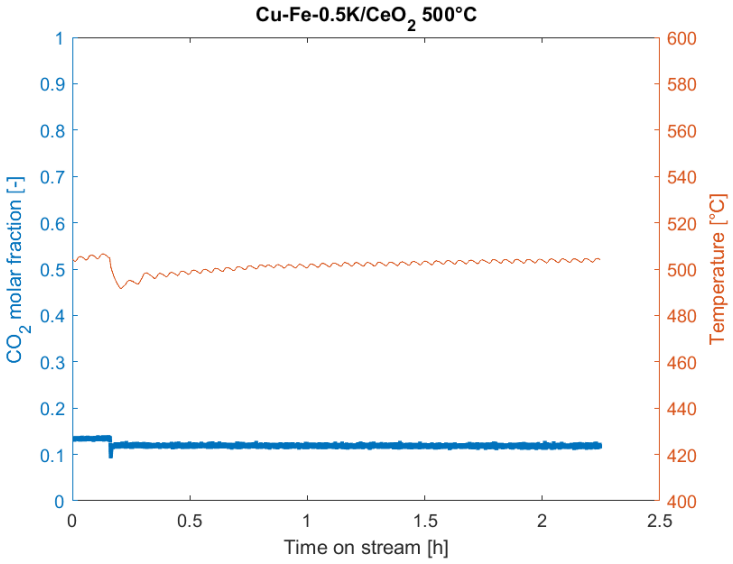
Cu-Fe-0.5K/CeO2 500°C
CO2 molar fraction [-]
Temperature [°C]
Time on stream [h]

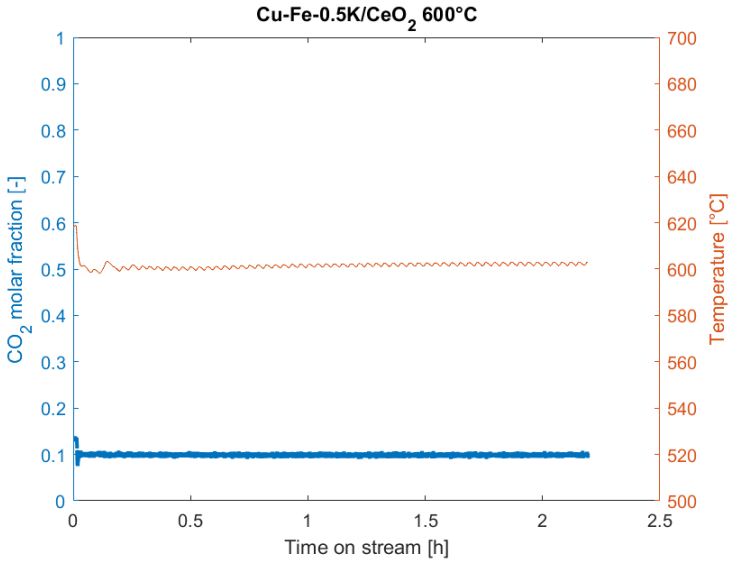
Cu-Fe-0.5K/CeO2 600°C
CO2 molar fraction [-]
Temperature [°C]
Time on stream [h]

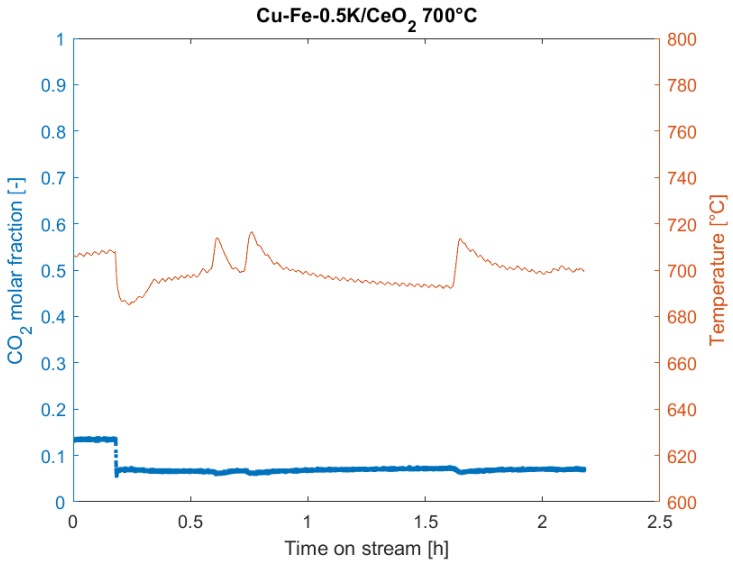
Cu-Fe-0.5K/CeO2 700°C
CO2 molar fraction [-]
Temperature [°C]
Time on stream [h]

A.3. Cu-Fe-1.9K/CeO_2

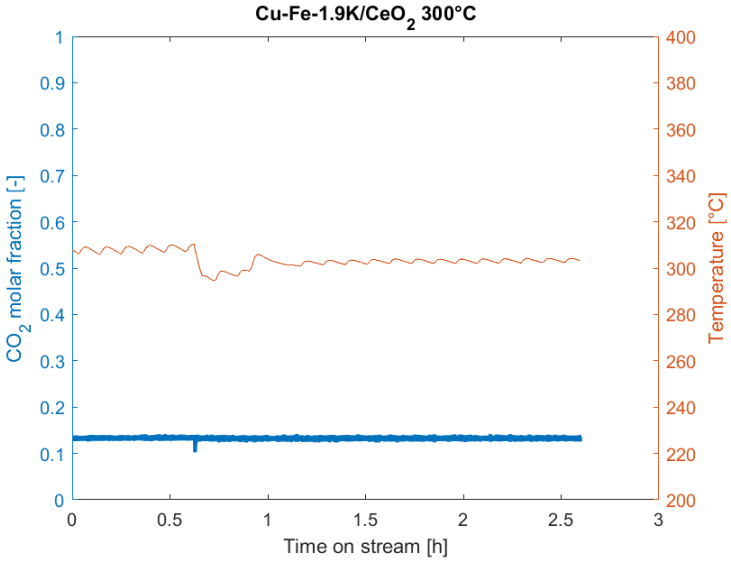

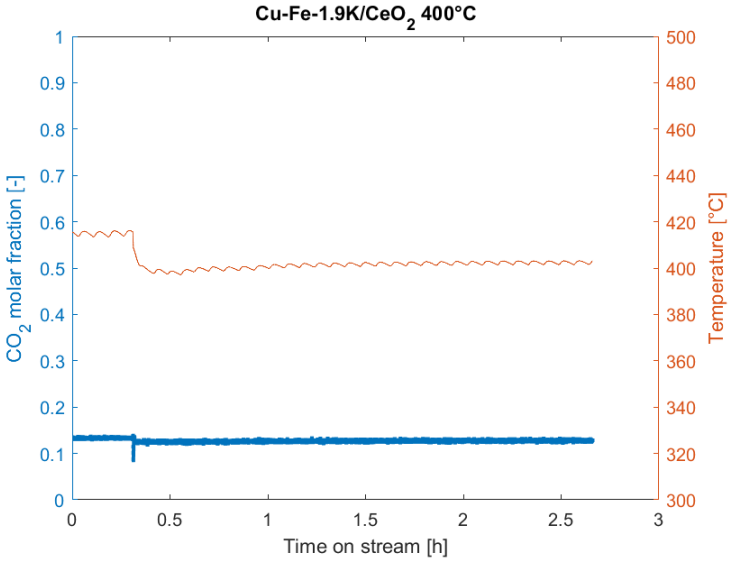

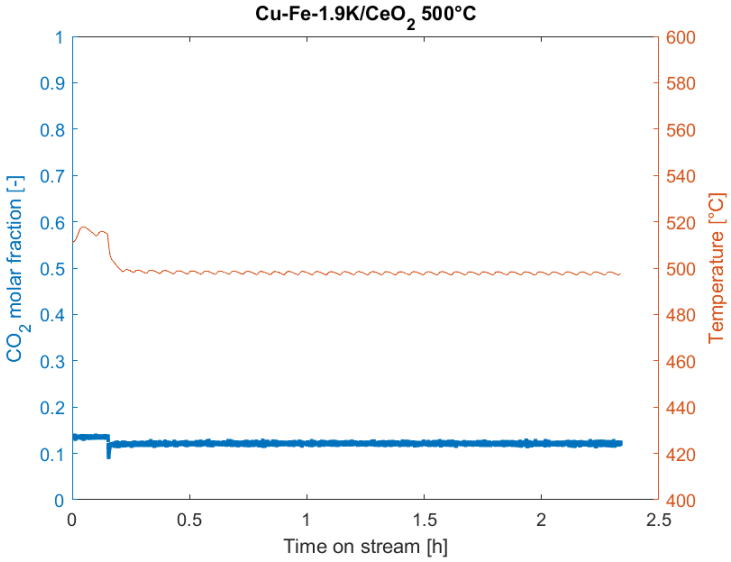

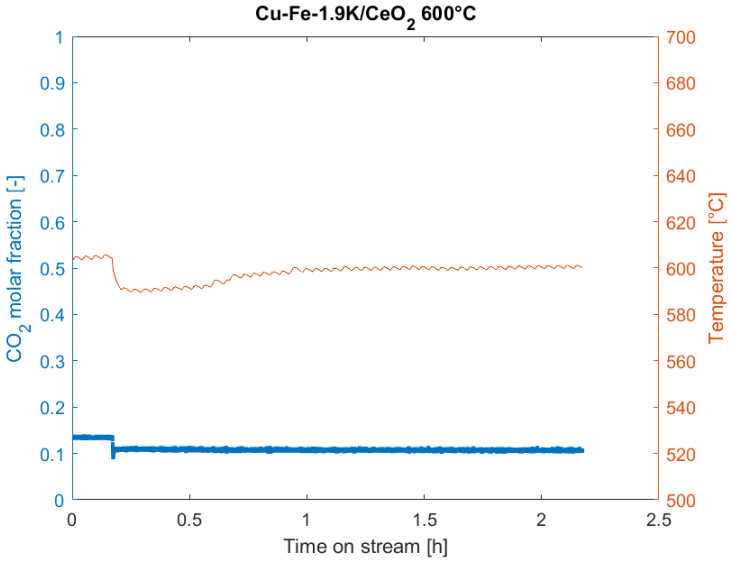

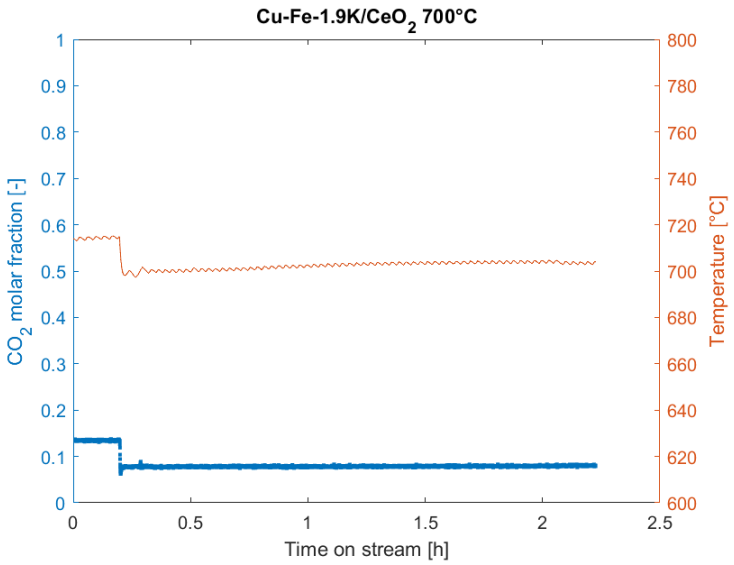
Cu-Fe-1.9K/CeO2 700°C
CO2 molar fraction [-]
Temperature [°C]
Time on stream [h]
0
0.1
0.2
0.3
0.4
0.5
0.6
0.7
0.8
0.9
1
600
620
640
660
680
700
720
740
760
780
800
0
0.5
1
1.5
2
2.5

List of Figures

List of Tables

List of Symbols

Variable	Description	SI unit
ΔH	enthalpy variation	J/mol
K_{eq}	equilibrium constant	-
ΔG_R^0	standard Gibbs reaction energy variation	J/mol
R	molar gas constant	J/mol/K
T	temperature	K
P^0	reference pressure	Pa
ν	stoichiometric coefficient	-
ΔG_f^0	standard Gibbs formation energy variation	J/mol
a	activity coefficient	Pa
x	molar fraction	-
K_{att}	activity constant	-
$D_{reactor}$	reactor diameter	m
D_p	particle diameter	m
X	conversion	-
S	selectivity	-
$\dot{n}$	molar flow	mol/s

Acknowledgements

Thanks to Prof. Lietti for giving me the opportunity to carry on my thesis work abroad, experiencing a new academic context.
Thanks to Efthymios for being my guide throughout this work. He has been a very competent and dedicated professor, while at the same time he always tried to bring up the fun side of work.
Thanks to Lars who invited me in the first place to KTH, where I had this incredible experience.
Finally, thanks to all the friends at the Process Technology division of KTH who welcomed me and made feel at home.